TORC2-dependent protein kinase Ypk1 phosphorylates ceramide synthase to stimulate synthesis of complex sphingolipids

Alexander Muir[1,2], Subramaniam Ramachandran[1], Françoise M. Roelants[1], Garrett Timmons[3] and Jeremy Thorner[1]*

[1]Division of Biochemistry, Biophysics and Structural Biology, Dept. of Molecular and Cell Biology, [2]Chemical Biology Graduate Program, and [3]Dept. of Chemistry, University of California, Berkeley CA 94720-3202

Running Title: Control of sphingolipid biosynthesis

*To whom correspondence should be addressed:

Professor Jeremy Thorner
Division of Biochemistry, Biophysics and Structural Biology
Department of Molecular and Cell Biology
University of California at Berkeley
Room 16, Barker Hall
Berkeley, CA 94720-3202 USA
Phone: (510) 642-2558
FAX: (510) 642-6420
e-mail: jthorner@berkeley.edu

Abstract

Plasma membrane lipid composition must be maintained during growth and under environmental insult. In yeast, signaling mediated by TOR Complex 2 (TORC2)-dependent protein kinase Ypk1 controls lipid abundance and distribution in response to membrane stress. Ypk1, among other actions, alleviates negative regulation of L-serine:palmitoyl-CoA acyltransferase, upregulating production of long-chain base precursors to sphingolipids. To explore other roles for TORC2-Ypk1 signaling in membrane homeostasis, we devised a three-tiered genome-wide screen to identify additional Ypk1 substrates, which pinpointed both catalytic subunits of the ceramide synthase complex. Ypk1-dependent phosphorylation of both proteins increased upon either sphingolipid depletion or heat shock and was important for cell survival. Sphingolipidomics, other biochemical measurements and genetic analysis demonstrated that these modifications of ceramide synthase increased its specific activity and stimulated channeling of long-chain base precursors into sphingolipid end-products. Control at this branch point also prevents accumulation of intermediates that could compromise cell growth by stimulating autophagy.

Introduction

A eukaryotic plasma membrane (PM) is a complex structure composed of many protein (Sachs and Engelman 2006) and lipid (Simons and Sampaio 2011) species arranged with a high degree of compositional and spatial organization. The levels and distributions of lipids are clearly important for PM processes— from solute transport (Divito and Amara 2009), to endocytosis (Platta and Stenmark 2011), to receptor function and signal transduction (Groves and Kuriyan 2010). It is essential, therefore, for a cell to maintain proper lipid balance. How cells sense alterations in PM organization in response to developmental cues or environmental stresses and adjust the rates of the reactions that maintain lipid homeostasis are vital mechanisms to understand.

We (Roelants et al. 2011) and others (Berchtold et al. 2012; Niles and Powers 2012) have shown that dynamic changes in the function of Target of Rapamycin (TOR) Complex 2 (TORC2) and in a downstream protein kinase that it stimulates, Ypk1 (and its paralog Ypk2), are important for cell survival in response to membrane stress. Ypk1 (and Ypk2) are two members of the AGC kinase family (Pearce et al. 2010) and orthologs of mammalian SGK1 (Casamayor et al. 1999). In *S. cerevisiae*, Ypk1 (and Ypk2) are activated at a basal level by phosphorylation of a Thr in the activation loop by the eisosome-associated protein kinase Pkh1 (and its paralog Pkh2) (Casamayor et al. 1999; Roelants et al. 2002). The ortholog responsible for this reaction in mammalian cells is PDK1 (Mora et al. 2004). However, this level of activity is not sufficient for Ypk1 to permit survival when cells are challenged with certain membrane perturbants (Roelants et al. 2004). Under such conditions of membrane stress, TORC2 stimulates Ypk1 and Ypk2 function by phosphorylating at least two C-terminal sites (Kamada et al. 2005; Roelants et al. 2011; Niles et al. 2012). Constitutively-active Ypk1 and Ypk2 alleles bypass the need for functional TORC2, indicating that Ypk1 and Ypk2 are solely responsible for executing all the essential downstream functions of TORC2 (Kamada et al. 2005; Roelants et al. 2011; Niles et al. 2012).

How membrane stress is communicated to TORC2 is a question of on-going research. It has been reported that membrane stress caused by inhibition of sphingolipid synthesis or membrane stretch (induced by hypotonic shock) causes two PH domain-containing proteins (Slm1 and Slm2) to relocalize from eisosomes to a separate PM region that contains TORC2 and leads to increased TORC2 activation of Ypk1 and Ypk2 (Berchtold et al. 2012), purportedly because Slm1 and Slm2 recruit Ypk1 and Ypk2 to TORC2 (Niles et al. 2012). However, other evidence indicates that Avo1 (ortholog in other organisms is Sin1) is the subunit of the TORC2 complex primarily responsible for substrate recognition of Ypk1 and its orthologs, including association of *S. cerevisiae* Ypk2 with Avo1 (Liao and Chen 2012), Gad8 with Sin1 in fission yeast (Ikeda et al. 2008; Kataoka et al. 2014), and SGK1 with mSin1 in mammalian cells (Jacinto et al. 2006; Yang et al. 2006; Lu et al. 2011; Liu et al. 2013). Regardless of the actual mechanism by which the activity of the TORC2-Ypk1 signaling module is affected by these assaults on the PM, it clearly sets in motion processes that allow the cells to cope appropriately with these stresses.

Several targets of Ypk1 have already been identified that shed light on how TORC2-Ypk1 signaling reprograms cellular processes to cope with PM stress. Ypk1 phosphorylates and negatively regulates Fpk1, a protein kinase responsible for activation of PM-localized aminophospholipid flippases (Roelants et al. 2010), thereby fine-tuning the phosphatidyl-ethanolamine content of the inner leaflet of the PM bilayer. Ypk1 also phosphorylates and alleviates the inhibitory function of two endoplasmic reticulum (ER)-localized proteins (Orm1 and Orm2) that impede the function of the first enzyme unique to sphingolipid biosynthesis, L-serine:palmitoyl-CoA acyltransferase (SPT) (Roelants et al. 2011; Berchtold et al. 2012; Sun et al. 2012), thereby increasing the rate of formation of the long-chain base precursor (phytoshingosine) to yeast sphingolipids. Ypk1 also phosphorylates and inhibits one of the two isoforms (Gpd1) of glycerol-3-phosphate dehydrogenase, a primary source of glycerol-3P for production of glycerophospholipids (Lee et al. 2012b). In response to hyperosmotic shock, and

in contrast to other PM stressors, TORC2 activity is markedly decreased, preventing Ypk1-mediated inhibition of Gpd1 [which also gets upregulated transcriptionally (Ansell et al. 1997)], thereby greatly increasing synthesis of glycerol-3P, which is dephosphorylated to produce glycerol, an inocuous osmolyte that yeast cells accumulate as a means to counteract the increase in external osmotic pressure (Lee et al. 2012b). Control of all these reactions already made it clear that TORC2-Ypk1 signaling is a central regulator of PM lipid homeostasis.

To gain further insight into how the TORC2-Ypk1 signaling axis contributes to PM homeostasis and potentially other cellular processes, we devised a three-step procedure to screen in an unbiased and genome-wide manner for additional candidate Ypk1 substrates whose physiological relevance we could then evaluate. As described here, we first used bioinformatics to search the yeast proteome for presumptive targets, then applied a genetic method to narrow down the hits to likely, functionally important substrates, and then used biochemical analysis both *in vitro* and *in vivo* to validate the best prospects. Although we report here the general outcomes of this screen, we focus mainly on our discovery and demonstration that both of the catalytic subunits of the ER-localized ceramide synthase complex (Schorling et al. 2001; Vallée and Riezman 2005) are *bona fide* targets of Ypk1. These findings provide new insight into how TORC2-initiated signaling regulates flux through the sphingolipid pathway and how this specific control mechanism is important for survival when sphingolipid synthesis is compromised. In addition, we show that this regulation of the ceramide synthase complex is important for preventing accumulation of pathway intermediates that would otherwise compromise cell growth by triggering an inappropriate autophagic response.

Results

A three-tiered screen to identify new Ypk1 substrates

We devised a three-step strategy (Fig. 1A) to pinpoint *bona fide* cellular targets of Ypk1, utilizing bioinformatics to predict potential Ypk1 substrates, then an *in vivo* genetic test involving a novel variation of the synthetic dosage lethality method to winnow the list to likely candidates, and finally biochemical analysis *in vitro* to confirm whether the identified gene product serves as a direct substrate of Ypk1. The physiological relevance of Ypk1-dependent modification of each protein on the resulting final list could then been evaluated.

For initial bioinformatic search of the yeast proteome, we developed a position-weighted consensus sequence logo (Fig. 1B) for the preferred Ypk1 phospho-acceptor site based on two primary criteria: (a) the known Ypk1 sites in five, validated *in vivo* targets (Fpk1, Fpk2, Orm1, Orm2, and Gpd1) (Roelants et al. 2010; Roelants et al. 2011; Lee et al. 2012b; Niles et al. 2012; Sun et al. 2012); and, (b) the sequence preference displayed by Ypk1 for phosphorylation of synthetic peptides *in vitro* (Casamayor et al. 1999; Mok et al. 2010). All demonstrated substrates either *in vivo* or *in vitro* contain Arg at positions -5 and -3 with respect to the phosphorylated Ser (or Thr); thus, these positions were invariant in the search motif. Given that nearly all the verified sites within known *in vivo* targets possess a hydrophobic residue (V, I, F) at position +1, the search motif gave preference to sites with a hydrophobic residue at the +1 position. We then took advantage of the existing MOTIPS motif analysis package (Lam et al. 2010) to identify those *S. cerevisiae* gene products that contain occurrences of the search logo. Several authentic Ypk1 substrates (*e.g.,* Fpk1, Orm1, and Orm2) contain multiple Ypk1 phosphorylation sites. Thus, we filtered our search further by prioritizing candidates containing multiple matches to the search logo, as predicted by MOTIPS. However, to avoid disregarding potential Ypk1 substrates with a single predicted match to the sequence logo, we also considered MOTIPS hits wherein there was existing evidence in the PhosphoGRID database (Sadowski et al. 2013) indicating that a predicted site is phosphorylated *in vivo*. To narrow down

the list of potential substrates further, we chose to pursue those gene products containing matches to the sequence logo for which there was existing information in the literature suggesting a phenotypic relationship to known Ypk1-dependent processes: (a) a loss-of-function mutation in the candidate gene exhibits elevated sensitivity to agents (aureobasidin A, caspofungin, and/or myriocin) toward which a *ypk1*Δ mutant is also sensitive (Hillenmeyer et al. 2008); (b) the candidate gene product is reported to be involved in a genetic or biochemical interaction with Ypk1, as curated in YeastMine (Balakrishnan et al. 2012); (c) the candidate gene product is connected in some way to known Ypk1 regulators (*e.g.*, TORC2, PP2A); and/or, (d) the candidate gene product is involved in a known Ypk1-regulated process (*e.g.*, sphingolipid metabolism) (for further details, see Materials and Methods). Reassuringly, our approach identified three known Ypk1 substrates (Fpk1, Orm1 and Orm2); absence of Fpk2 and Gpd1 from the list generated solely by the MOTIPS search criteria arose from the fact that these substrates contains only a single predicted site that is not presently recorded in PhosphoGRID. For this reason, we also restored for consideration additional gene products that contain a single match to the consensus sequence logo that YeastMine indicated are involved in processes in which Ypk1 is implicated. The resulting candidates, grouped via cellular process on the basis of current GO Slim terminology (http://www.geneontology.org/GO.slims.shtml), are cataloged in Table 1, and represent fewer than 100 gene products out of the approximately 6,000 protein-coding genes in the yeast genome (Lin et al. 2013) [although the number of authentic open-reading-frames undergoes constant revision (http://www.yeastgenome.org/cache/genomeSnapshot.html)].

As the secondary filter for the candidates recognized bioinformatically, we developed an *in vivo* approach to identify those gene products that manifested an expected hallmark of protein-substrate interaction. We reasoned that under conditions where the level of activity of an essential kinase, like Ypk1, is near-limiting for normal growth, high-level over-expression of an authentic substrate might tie up the available pool of active enzyme and prevent efficient

phosphorylation of other cellular substrates necessary for growth and/or viability (Fig. 1C). This scheme is a novel variation on a genetic approach referred to as synthetic dosage lethality (SDL) (Sopko et al. 2006; Sharifpoor et al. 2012). To limit Ypk1 activity, we used *ypk1-as ypk2*Δ cells, which express from the *YPK1* locus an analog-sensitive allele, Ypk1(L424A) (Roelants et al., 2011; Niles et al., 2012), and titrated down its activity by addition of a low concentration of an efficacious inhibitor,1-(*tert*-butyl)-3-(3-methylbenzyl)-1H-pyrazolo[3,4-d]pyrimidin-4-amine (3-MB-PP1) (Burkard et al. 2007) that has no effect on wild-type cells (see Fig. 2C). To achieve high-level over-expression, each bioinformatic hit was expressed from the galactose-inducible *GAL1* promoter on a *CEN* plasmid. As proof of concept, we used two known Ypk1 substrates, Orm1 and Orm2, as positive controls and GFP, which is not a Ypk1 substrate (data not shown), as a negative control. In the absence of limiting the activity of Ypk1(L424A) with inhibitor, overexpression of neither Orm proteins nor GFP was deleterious to cell growth (Fig, 1D, *left panels, compare lower to upper*). However, in the presence of a low dose of 3-MB-PP1, overexpression of Orm1 and Orm2 on galactose medium prevented cell growth, whereas overexpression of GFP did not (Fig. 1D, *middle and right panels, compare lower to upper*). We were able to test the majority of the candidates (90/96) that arose in the bioinformatic search in this same fashion [however, 10/90 caused toxicity upon over-expression even in wild-type cells and, hence, could not be scored].

Those candidates that, like Orm1 and Orm2, exhibited toxicity only on galactose medium and only when Ypk1(L424A) activity was limited in the presence of 3-MB-PP1, but not when inhibitor was absent, were designated SDL hits (Table 1, *column 4*). Moreover, use of a series of 3-MB-PP1 concentrations allowed for quantification of the strength of the SDL effect (from + to ++++). In one case (Fps1), a marked SDL effect was observed upon overexpression in the *ypk1-as ypk2Δ* cells in the absence of chemical inhibition; we considered this a valid SDL hit because *GAL* promoter-driven over-expression of Fps1 was not growth inhibitory in wild-type (*YPK1*$^{+}$ *YPK2*$^{+}$) cells. Thus, as summarized in Table 1 (*column 4*), a significant fraction (20/90)

of the candidates identified bioinformatically that were tested in this fashion, but far from all, displayed an SDL phenotype. In this regard, it is important to note that all known Ypk1 substrates tested (Gpd1, Fpk1, Orm1 and Orm2) displayed an SDL phenotype, whereas nearly 80% of the bioinformatic hits, like GFP, did not. Consistent with the view that the SDL phenotype could arise from the over-expressed target serving as a decoy substrate that titers a limited pool of active Ypk1 away from acting on its essential substrates, we observed that over-expressed catalytically-inactive Fpk1 caused an SDL phenotype equivalent to or stronger than wild-type Fpk1 (Table 1). If such SDL phenotypes reflect occlusion of a limited pool of enzyme by over-expressed substrate, then, conversely, co-overexpression of Ypk1 or even of a kinase-dead allele Ypk1(K376A) (driven from the *MET25* promoter) might rescue the toxicity. Indeed, the deleterious effect of Smp1 over-expression was rescued by co-over-expression of either Ypk1 or Ypk1(K376A) (Table 1), suggesting that the SDL phenotype of over-expressed Smp1 also arises from titration of a limited amount of Ypk1 away from essential substrates.

Lastly, to determine whether the gene products that displayed an SDL phenotype are indeed substrates for Ypk1, we incubated those (17/20) that we were able to successfully express and purify as recombinant proteins or protein fragments (as GST fusions) from *E. coli* with [γ-^{32}P]ATP and Ypk1(L424A), which was highly purified from yeast cells as described in Materials and Methods. We chose to use the analog-sensitive allele, even though it is only about 50% as active as wild-type Ypk1 (Roelants et al. 2011), because ablation of activity in the presence of 3-MB-PP1 allowed us to confirm that any ^{32}P incorporation into substrate observed was due to phosphorylation by Ypk1(L424A) itself (and not due to some other protein kinase that might be present in the preparation). All known *in vivo* substrates of Ypk1 (Fpk1, Fpk2, Gpd1, Orm1 and Orm2) display robust incorporation (as judged by autoradiography) in this *in vitro* assay (Roelants et al. 2010; Roelants et al. 2011; Lee et al. 2012b). Therefore, in testing each candidate, an appropriate positive control, Orm1(1-85) was included (Fig. 1E), which also allowed comparison between independent assays. Gratifyingly, 12/17 (70%) of the SDL hits

tested in this manner displayed readily detectable and Ypk1-specific phosphorylation (Table 1, *right column*). Moreover, the results of such assays clearly demonstrated that Ypk1 is not a "promiscuous" enzyme. For example, Fps1 has three possible N-terminal Ypk1 sites (**R**P**R**GQ**T**^{147}T, **R**R**R**SR**S**^{181}R and **R**S**R**AT**S**^{185}N) and one C-terminal site. The C-terminal site is a Ypk1 target (data not shown); however, none of the N-terminal motifs serves as a Ypk1 phospho-acceptor site (Fig. 1E), most likely because each lacks a hydrophobic residue at +1.

Thus, we considered it very likely that the dozen candidates identified bioinformatically that also displayed an SDL phenotype and served as Ypk1 substrates *in vitro* (highlighted in bold in Table 1) would be functionally important Ypk1 substrates *in vivo*. To validate this conclusion and confirm that these candidates are indeed physiologically relevant Ypk1 targets, we chose to characterize Lac1 and Lag1, two of the dozen candidates (Table 1), because they are the catalytic subunits of the ceramide synthase complex and might further our understanding about how sphingolipid production is regulated by the TORC2-Ypk1 signaling axis.

Ceramide synthase components Lac1 and Lag1 are identified as Ypk1 substrates

Lac1 (418 residues) and Lag1 (411 residues) are apparent paralogs at the primary sequence level (69% identity, 77% similarity) (Byrne and Wolfe 2005) and are polytopic integral proteins in the ER membrane with the predicted Ypk1 site in each protein residing near its N-terminus (Fig. 2A). It has been shown that the N-termini of these proteins are exposed to the cytosol (Kageyama-Yahara and Riezman 2006). Along with a small accessory subunit Lip1 (150 residues), Lac1 and Lag1 are demonstrated constituents of the ceramide synthase complex (Schorling et al. 2001; Vallée and Riezman 2005), which catalyzes N-acylation of the free amino group on the long-chain base (LCB), mainly phytosphingosine in yeast, using fatty acyl-CoA as the acyl donor, thereby forming phytoceramide (Fig. 2B). Genetically, Lac1 and Lag1 appear to play overlapping functional roles; *lac1Δ* or *lag1Δ* single mutants are viable, whereas a *lac1Δ lag1Δ* double mutant is reportedly either inviable (Jiang et al. 1998) or extremely slow growing (Barz and Walter 1999; Schorling et al. 2001; Vallée and Riezman 2005). The ceramide

synthase reaction lies at an important branch point in the sphingolipid metabolic network (Fig. 2B) because *de novo* synthesis of ceramides both consumes LCBs and prevents conversion of LCBs to their 1-phosphorylated derivatives (LCBPs). Thus, the rate of ceramide synthesis is tightly coupled to the levels of both LCBs and LCBPs (Kobayashi and Nagiec 2003); and, moreover, the balance between ceramides and total LCBs and LCBPs affects growth rate in both fungi (Kobayashi and Nagiec 2003) and mammalian cells (Spiegel and Milstien 2003). By virtue of their position in the pathway, Lac1 and Lag1 are situated to be important regulators of this balance.

Among the bioinformatically predicted substrates, both Lac1 and Lag1 displayed a readily detectable SDL phenotype (Fig. 2C) and both GST-Lac1(1-76) and GST-Lag1(1-80) served as *in vitro* substrates for Ypk1, albeit with the phosphorylation of Lac1 being reproducibly much more robust than Lag1 (Fig. 2D). Site-directed mutagenesis confirmed that the Ypk1-mediated phosphorylation of both substrates occurred exclusively at the predicted phospho-acceptor site(s), specifically Ser23 and Ser24 in both proteins (Fig. 2D).

***Lac1 and Lag1 are phosphorylated by Ypk1* in vivo**

To determine whether both Lac1 and Lag1 are phosphorylated *in vivo* in a Ypk1-dependent manner and at their Ypk1 consensus sites, an integrated 3xHA-tagged version of each protein and its corresponding S23A S24A mutant was expressed in yeast and extracts of the cells were analyzed by phosphate-affinity SDS-PAGE (Phos-tag gels) (Kinoshita et al. 2009). In this separation technique, the more highly phosphorylated the protein, the more its migration is retarded. Both Lac1 (Fig. 3A, *left*) and Lag1 (Fig. 3A, *right*) migrated as two species, and the slower of the two could be attributed to phosphorylation because it was eliminated if the sample was pre-treated with calf intestinal phosphatase. This slower mobility species represented phosphorylation at S23 and S24 because the band was also eliminated in Lac1(S23A S24A) and Lag1(S23A S24A) mutants (Fig. 3A). We noted that phosphatase treatment, even of the Lac1(S23A S24A) and Lag1(S23A S24A) mutants, resulted in appearance of a third, even faster

migrating species, presumably due to removal of a phosphorylation(s) elsewhere in these proteins, consistent with indirect evidence that Lac1 and Lag1 might be subject to casein kinase II (yeast Cka2)-dependent modification (Kobayashi and Nagiec 2003).

In agreement with their relative efficacies as *in vitro* substrates (Fig. 2D), we found that, reproducibly, the majority of Lac1 was present in the cell as the slower mobility isoform, whereas the opposite was true for Lag1 (Fig. 3A). Because the behavior of Lac1 gave us greater sensitivity of detection, and for the sake of conciseness, some of our subsequent findings are illustrated with data for Lac1 only. However, all experiments were repeated with both proteins with virtually identical results and conclusions.

To further confirm that Ypk1 is the protein kinase responsible for phosphorylation at Ser23 Ser24 *in vivo*, plasmids encoding 3xHA-tagged tagged Lac1 and Lag1 were introduced by DNA-mediated transformation into wild-type, *ypk1Δ*, and *ypk2Δ* strains. Cultures of the resulting cells were grown in the absence or presence of a sub-lethal dose of myriocin, a condition which several previous studies have shown activates TORC2- and Ypk1-mediated signaling (Roelants et al. 2011; Berchtold et al. 2012; Sun et al. 2012), and the resulting extracts were analyzed on Phos-tag gels. As observed previously for two other *bona fide* substrates, Orm1 and Orm2 (Roelants et al. 2011), absence of Ypk1 totally abrogated the appearance of phosphorylated Lac1 (Fig. 3B) and phosphorylated Lag1 (data not shown), whereas elimination of Ypk2 had no effect. Thus, Ypk1 is the paralog solely responsible for the observed *in vivo* phosphorylation of Lac1 and Lag1 at Ser23 and Ser24. Furthermore, under conditions that stimulate TORC2 activity, nearly all of the Lac1 (Fig. 3B) and much more of the Lag1 (data not shown) were converted to the phosphorylated isoform indicating that TORC2 activation is relayed to ceramide synthase via Ypk1. To further confirm that TORC2 function is essential for Ypk1-mediated phosphorylation of ceramide synthase, Lac1 phosphorylation was monitored in *TOR2* cells and in a *tor2-as* mutant after addition of a specific *tor2-as* inhibitor, BEZ-235 (Kliegman et al. 2013). TORC2 inhibition markedly reduced Lac1 phosphorylation within 20 min in *tor2-as* cells, but not

297 in the otherwise isogenic control cells (Fig. 3C), confirming that TORC2 activity is necessary for
298 Ypk1-mediated ceramide synthase phosphorylation. Thus, our screening approach was
299 successful in revealing two, previously uncharacterized, cellular targets of the TORC2-Ypk1
300 signaling axis.

301 **Increased Lac1 and Lag1 phosphorylation is required for cell survival under stress**

302 The fact that impeding LCB production with a sub-lethal dose of the SPT inhibitor myriocin
303 stimulated Ypk1-mediated Lac1 and Lag1 phosphorylation suggested that this modification is
304 important for their physiological function. As one means to confirm that reduction in sphingolipid
305 biosynthesis capacity results in up-regulation of Lac1 and Lag1 phosphorylation, we subjected
306 the pathway to blockade near its end by treating the cells expressing integrated 3xHA-tagged
307 Lac1 or Lag1 with aureobasidin A (Heidler and Radding 1995), an antibiotic that prevents
308 formation of complex sphingolipids in yeast by inhibiting Aur1 (phosphatidylinositol:ceramide
309 phosphoinositol transferase) (Nagiec et al. 1997). As observed for treatment with myriocin, the
310 amount of phosphorylated Lac1 (Fig. 4A) and Lag1 (data not shown) was markedly increased in
311 response to treatment with aureobasidin A.

312 Another perturbation that has been shown to transiently up-regulate TORC2-Ypk1-mediated
313 signaling is heat shock (Sun et al. 2012). Consistent with that response, it has been shown
314 previously that heat shock leads to a transient increase in sphingolipid production and that
315 sphingolipid production is important for heat shock survival (Jenkins et al. 1997; Cowart et al.
316 2003). Moreover, measurement of pathway intermediates and mathematical modeling also
317 suggested that a sharp spike of increased ceramide synthase activity may occur after heat
318 shock (Chen et al. 2013). Therefore, we subjected the same cells to heat shock and monitored
319 Lac1 and Lag1 phosphorylation at various times thereafter. Within 5 min, the amount of
320 phosphorylated Lac1 (Fig. 4B) and Lag1 (data not shown) increased markedly, but was back to
321 the resting level by 30 min.

322 If these changes in phosphorylation state at Ser23 and Ser24 in Lac1 and Lag1 are

important for the metabolic adjustments that the cell needs to adapt appropriately, then preventing phosphorylation at these sites should impair cell survival. To test this prediction, we integrated as the sole source of ceramide synthase, mutant versions of Lac1 and Lag1 in which Ser23 and Ser24 were mutated to Ala and, hence, cannot be phosphorylated under any circumstances. As a control, we also generated integrated versions of Lac1 and Lag1 in which Ser23 and Ser24 were mutated to Glu, to mimic conversion of the entire population to the phosphorylated state, a response that we showed can be achieved for the wild-type protein (see, for example, Fig. 3B). Indeed, we found that the cells co-expressing Lac1(S23A S24A) and Lag1(23A S24A) grew detectably less well when challenged with either myriocin or aureobasidin A than either otherwise isogenic wild-type cells or cells co-expressing Lac1(S23E S24E) and Lag1(S23E S24E) (Fig. 4C). These growth differences could not be attributed to differences in the level of expression of these proteins, as immunoblot analysis demonstrated the wild-type and mutant ceramide synthase subunits were present in equivalent amounts under the conditions tested (Fig. 4D). Thus, Ypk1-dependent phosphorylation of these sites in Lac1 and Lag1 is functionally important for cell survival in response to the stress of limiting sphingolipid biosynthesis. Furthermore, the fact that the Lac1(S23E S24E) Lag1(S23E S24E) strain phenocopied a *LAC1*$^{+}$ *LAG1*$^{+}$ strain under conditions that promote phosphorylation of Lac1 and Lag1 indicates that these mutations generated effective phosphomimetic alleles.

Calcineurin down-regulates Lac1 and Lag1 phosphorylation at Ser23 and Ser24

As a means to delineate what cellular phosphatase is responsible for counteracting the Ypk1-mediated phospho-regulation of Lac1 and Lag1, plasmid-borne 3xHA-tagged Lac1 was expressed in a collection of deletion strains lacking each of the non-essential protein phosphatase genes or their associated factors, and the phosphorylation state of Lac1 was assessed using Phos-tag gels. By this approach, we were unable to find any phosphatase-deficient mutant that exhibited a significant increase in the amount of phosphorylated Lac1 compared to control cells (data not shown). However, considerable genetic evidence indicates a

strong connection between Ca^{2+} signaling and sphingolipid biosynthesis (Beeler et al. 1998). Moreover, it has been reported previously that TORC2-Ypk-dependent regulation of sphinglipid biosynthesis is antagonized by the action of the Ca^{2+}/calmodulin-dependent protein phosphatase calcineurin (also known as phosphoprotein phosphatase 2B), although the level at which the phosphatase acted was unknown (Aronova et al. 2008). Hence, we conducted the converse experiment by stimulating the cells expressing 3xHA-tagged Lac1 acutely with 0.2 M $CaCl_2$, a condition known to robustly activate calcineurin in yeast (Stathopoulos-Gerontides et al. 1999). Within <10 min, we found total abrogation of phospho-Lac1 (Fig. 5A, *left*) and total abrogation of phospho-Lag1 (data not shown) in wild-type cells, whereas in otherwise isogenic *cna1Δ cna2Δ* mutants (which lack both calcineurin catalytic subunit paralogs) a substantial portion of the phosphorylated species remained (Fig. 5A, *right*).

These results suggested that calcineurin may directly reverse the phoshorylations introduced into Lac1 and Lag1 by Ypk1. However, it is also the case that two of the ancillary subunits associated with TORC2, Slm1 and Slm2, are demonstrated calcineurin-binding proteins (Bultynck et al. 2006; Tabuchi et al. 2006) and that calcineurin action appears to oppose TORC2-dependent signaling (Mulet et al. 2006; Daquinag et al. 2007; Berchtold et al. 2012). Hence, it was possible, therefore, that the observed loss of phospho-Lac1 and -Lag1 might be due to a Ca^{2+}-stimulated and calcineurin-mediated reduction in their TORC2-Ypk1-dependent phosphorylation, rather than to direct action of calcineurin on phospho-Lac1 and -Lag1. To rule out the former possibility, we examined Lac1 and Lag1 phosphorylation in cells expressing constitutively-active Ypk1(D242A), which we have demonstrated bypasses the need for its TORC2-dependent activation (Roelants et al. 2011). We found that Ca^{2+} addition still led to nearly complete Lac1 and Lag1 dephosphorylation in these cells (Fig. 5B). Furthermore, as judged by immunoblotting with a phospho-site specific antibody, Pkh1- and Pkh2-dependent phosphorylation of the activation loop in Ypk1 (Fig. 5C) [or in Ypk1(D242A) (data not shown)] was not diminished in cells stimulated with Ca^{2+}, confirming that there was no calcineurin-

mediated decrease in the amount of active Ypk1 present. Therefore, it seems clear that calcineurin dephosphorylates the sites in Lac1 and Lag1 phosphorylated by Ypk1 directly, rather than through down-regulation of Ypk1 function.

Ypk1-mediated phosphorylation of Lac and Lag1 stimulates ceramide synthase activity

Given the phenotypic evidence that TORC2-Ypk1-dependent modulation of Lac1 and Lag1 is physiologically important (Fig. 4C), we next conducted biochemical analysis to determine how Ypk1-mediated phosphorylation affects the function of Lac1 and Lag1 in ceramide synthesis. Toward that end, we first used LC-MS to monitor the levels of LCBs and LCBPs extracted from equivalent numbers of cells from exponentially-growing cultures of wild-type cells or otherwise isogenic cells expressing as the sole source of Lac1 and Lag1 either the non-phosphorylatable Lac1(S23A S24A) and Lag1(S23A S24A) mutants or the phosphomimetic Lac1(S23E S24E) and Lag1(S23E S24E) mutants. Relative to wild-type cells, the Lac1(S23A S24A) Lag1(S23A S24A) cells accumulated significantly more PHS (Fig. 6A, *top left*), as well as more dihydrosphingosine (DHS) (Fig. 6A, *top right*), which is a more minor LCB in yeast (note the difference in scale of the ordinate), whereas the Lac1(S23E S24E) Lag1(S23E S24E) cells displayed a level of both PHS and DHS that was somewhat lower, and a similar trend was observed even for PHS-1P, an even less abundant metabolite (Fig. 6A, *bottom left*). The level of DHS-1P (Fig. 6A, *bottom right*) was so low as to make reliable measurement difficult, but no differences between strains could be detected. Given that the ceramide synthase complex is responsible for the conversion of LCBs into ceramides, these findings indicate that, in the absence of Ypk1-mediated phosphorylation, the rate of LCB utilization is significantly reduced, consistent with the conclusion that Ypk1-dependent modification of Lac1 and Lag1 promotes ceramide synthase function.

As an independent means to measure flux through the sphingolipid pathway, and because all complex sphingolipids in yeast contain inositol-phosphate, an equivalent number of cells of the same three strains in mid-exponential phase were pulse-labeled, in triplicate, with $[^{32}P]PO_4^{-3}$,

401 and the acidic sphingolipids extracted and analyzed by thin-layer chromatography. Strikingly,
402 the amount of complex sphingolipids generated during the pulse was reproducibly higher in the
403 Lac1(S23E S24E) Lag1(S23E S24E) cells than in the wild-type controls, and Lac1(S23A S24A)
404 Lag1(S23A S24A) generated levels of complex sphingolipids lower than the wild-type controls
405 (Fig. 6B). These findings are again consistent with the conclusion that Ypk1-mediated
406 phosphorylation of Lac1 and Lag1 stimulates the production of the ceramide precursors to
407 complex sphingolipids.

408 Ypk1-mediated phosphorylation could stimulate the ceramide synthase reaction *in vivo* by
409 stabiizing Lac1 and Lag1 thereby increasing their steady-state level, by enhancing their
410 association with the small ancillary subunit Lip1, and/or by direct activation. Immunoblotting of
411 exponentially-growing cultures expressing the 3xHA-tagged versions of wild-type Lac1 and
412 Lag1 and the Lac1(S23A S24A) Lag1(S23A S24A) and Lac1(S23E S24E) Lag1(S23E S24E)
413 indicated no discernible difference in their steady-state level (see Fig. 4D). Likewise, in cells co-
414 expressing the same proteins and FLAG-tagged Lip1 (gift of Howard Riezman, Univ. of
415 Geneva), we observed no difference in the efficiency of Lip1 co-immunoprecipitation between
416 wild-type Lac1 and Lag1 and either the Lac1(S23A S24A) Lag1(S23A S24A) or Lac1(S23E
417 S24E) Lag1(S23E S24E) mutants (data not shown). These results suggested that Ypk1-
418 mediated phosphorylation may directly enhance the catalytic efficiency of Lac1 and Lag1. To
419 test this possibility directly, 3xFLAG-tagged versions of Lac1 and Lag1 were immuno-purified
420 from detergent-solubilized microsomes isolated from exponentially-growing cells and equivalent
421 amounts of the resulting protein assayed *in vitro*, monitoring the formation of ceramide from
422 PHS and steroyl-CoA by LC-MS. No product was observed in the absence of added steroyl-
423 CoA (data not shown), and product formation was reduced by 85% in the presence of PHS and
424 steroyl-CoA if 1 μM australifungin, a demonstrated and specific ceramide synthase inhibitor
425 (Mandala and Harris, 2000), was added (data not shown), confirming that the reaction
426 measured was catalyzed by ceramide synthase. We found that the specific activity of the

Lac1(S23E S24E) Lag1(S23E S24E) complex was reproducibly ~2 higher than either the Lac1(S23A S24A) Lag1(S23A S24A) mutant or the wild-type complex (Fig. 6C, *upper panel*), similar to the degree of difference in sphingolipid metabolites between these same strains that we measured by other means (Fig. 6A and 6B). In two independent trials (each performed in triplicate), the identical trend was found when microsomes from these same cells were assayed directly (i.e. without detergent solubilization and enzyme enrichment by immunoprecipitation (data not shown). Additionally, we found that immunopurified ceramide synthase from wild-type cultures treated with myriocin had higher activity than ceramide synthase prepared from untreated cells (Fig. 6C, *lower panel*). Furthermore, this increase in ceramide synthase activity in response to myriocin treatment was not observed in Lac1(S23A S24A) Lag1(S23A S24A) cells (Fig. 6C, *lower panel*), consistent with TORC2-Ypk1 signaling increasing ceramide synthase activity by phosphorylation at these residues. These findings are also in agreement with a reported ~2 fold decrease in the rate of ceramide production by ceramide synthase complex isolated from TORC2-deficient yeast (Aronova et al. 2008). Hence, we conclude that Ypk1 phosphorylation directly increases the catalytic activity of ceramide synthase.

Ypk1-mediated stimulation of Lac1 and Lag1 prevents autophagy induction during TORC2-driven up-regulation of sphingolipid biosynthesis

The observed increase in ceramide synthase activity in response to Ypk1-mediated phosphorylation could serve two roles that are not mutually exclusive: (i) to produce more ceramide and the derived complex sphingolipids; and, (ii) to prevent inadvertent accumulation of LCBs and the derived LCBPs when TORC2-driven Ypk1 activation stimulates metabolic flow into the sphingolipid pathway by alleviating Orm1- and Orm2-imposed inhibition of SPT (see Fig. 8). We reasoned that if the latter were one of the important physiological functions of Ypk1-dependent stimulation of ceramide synthase, then TORC2 activation would be detrimental to cells in which the Lac1(S23A S24A) Lag1(S23A S24A) mutant is the sole source of this enzyme. To mimic TORC2-stimulated elevation of Ypk1 activity, the constitutively-active

Ypk1(D242A) allele (hereafter referred to as Ypk1*) was expressed from the *YPK1* promoter on a *CEN* plasmid in either wild-type cells or the Lac1(S23A S24A) Lag1(S23A S24A) mutant. Indeed, compared to the empty vector control, expression of Ypk1* was well tolerated by cells containing wild-type Lac1 and Lag1, but deleterious to the growth of the Lac1(S23A S24A) Lag1(S23A S24A) mutant cells, whether measured on agar plates (Fig. 7A, *top*) or in liquid culture (Fig. 7A, *bottom*).

Given that accumulation of LCBPs has been shown to be toxic to yeast cell growth (Kim et al. 2000), we reasoned that the most likely metabolic perturbation responsible for the observed decrease in growth in the Lac1(S23A S24A) Lag1(S23A S24A) cells expressing Ypk1* was the build-up of LCBs and derived LCBPs. Consistent with this conclusion, we found a reproducible and statistically significant increase in the LCBP level in Lac1(S23A S24A) Lag1(S23A S24A) cells, compared to *LAC1*$^{+}$ *LAG1*$^{+}$ controls, and a further increase in Lac1(S23A S24A) Lag1(S23A S24A) cells expressing Ypk1* (Fig. 7B). If accumulation of LCBPs in Lac1(S23A S24A) Lag1(S23A S24A) co-expressing Ypk1* is indeed responsible for the poor growth, then reduction in LCBP synthesis by elimination of the gene *LCB4*, which encodes the major LCB kinase (Nagiec et al. 1998), should alleviate the growth inhibition. As expected, introduction of an *lcb4*Δ null mutation into the Lac1(S23A S24A) Lag1(S23A S24A) mutant suppressed the growth inhibitory effect of Ypk1* (Fig. 7C). Conversely, and consistent with toxicity arising from accumulation of LCBPs when Lac1 and Lag1 cannot be stimulated by Ypk1, we found that the poor growth phenotype of cells lacking the gene (*LCB3*) encoding the major LCBP phosphatase (Mandala et al. 1998), was markedly exacerbated by introduction of the Lac1(S23A S24A) Lag1(S23A S24A) alleles, but not by introduction of the Lac1(S23E S24E) Lag1(S23E S24E) alleles (Fig. 7D). In fact, and strikingly, presence of the Lac1(S23E S24E) Lag1(S23E S24E) allele afforded nearly complete rescue of the slow-growth phenotype of the *lcb3*Δ mutation (Fig. 7D). Consistent with the toxicity of LCBPs when LCB utilization by ceramide synthase is inefficient, an *elo3* mutation, which prevents efficient formation of C_{26}-CoA (an acyl chain found

in yeast ceramides), was synthetically lethal with *lcb3*Δ (Kobayashi and Nagiec 2003).

Finally, it has been reported that aberrant increases in LCBP level impede growth by triggering autophagy even under nutrient-rich conditions (Zimmermann et al. 2013). In agreement with the poor growth arising from LCBP-evoked induction of autophagy, we found, first, that Lac1(S23A S24A) Lag1(S23A S24A) cells expressing Ypk1* exhibited a readily detectable increase in basal GFP-Atg8 processing, comparable to that in *lcb3*Δ cells (but, of course, much less than that occurring when cells were treated with the starvation mimetic rapamycin) (Fig. 7E). Second, we found that preventing autophagy by ablating the gene *ATG1*, which encodes a protein kinase necessary for induction of autophagophore formation and its elongation (Papinski and Kraft 2014), provided substantial rescue of the growth debilitating effect of Ypk1* expression in Lac1(S23A S24A) Lag1(S23A S24A) cells (Fig. 7F, compare to Fig. 7A). This rescue was not due to an indirect effect of the absence of Atg1 on LCBP level because introduction of the *atg1Δ* mutation did not prevent the observed hyper-accumulation of LCBP in Lac1(S23A S24A) Lag1(S23A S24A) cells expressing Ypk1* (Fig. 7G). Collectively, these results indicate that, aside from stimulating ceramide synthesis *per se*, another physiologically important role of Ypk1-dependent ceramide synthase activation is, at least in part, to prevent hyper-accumulation of LCBPs and thereby avoid inadvertent induction of autophagy under nutrient-sufficient conditions (Fig. 8).

Discussion

Identification of new TORC2-Ypk1 substrates

Our approach identified Lac1 and Lag1 as potential Ypk1 targets, and our subsequent characterization demonstrated unequivocally that both Lac1 and Lag1 are *bona fide* Ypk1 substrates *in vivo* and that their Ypk1-dependent modification is biologically important for optimal modulation of sphingolipid metabolism. These findings validate the ability of our methods for discovery of physiologically relevant protein kinase substrates. Phospho-acceptor site motif pattern-matching alone, although useful in identifying kinase substrates in some cases (Yaffe et al. 2001; Manning et al. 2002; Mah et al. 2005; Holt et al. 2007; Linding et al. 2007; Rennefahrt et al. 2007; Gwinn et al. 2008; Hutti et al. 2009), can yield a large number of false positives. This possibility was a significant concern for us because certain features of the basophilic Ypk1 motif are shared with other protein kinases (Mok et al. 2010). As a means to avoid this problem, we devised a novel SDL-based genetic approach to apply as a secondary filter to parse the bioinformatically selected candidates further.

Although not the only possible explanation for detecting an SDL hit, one mechanism our genetic method should be able to assess is whether the candidate gene product displays a primary characteristic of a true substrate, namely the ability to compete with other substrates for association with Ypk1. A genuine Ypk1 substrate should, when highly over-expressed, sequester a large fraction of the available pool of active kinase, and thus impede its actions on its essential cellular targets. In the absence of Ypk2, over-expression of an authentic Ypk1 substrate should therefore be deleterious for growth when the activity of an analog-sensitive Ypk1 allele is reduced with a selective inhibitor. The fact that 70% of the SDL hits were indeed substrates for Ypk1-mediated phosphorylation *in vitro* verified that our use of this genetic method as a secondary filter to pick out true substrates from the list of bioinformatically identified candidates was well justified. In this regard, overexpression of Fpk1(KD), a catalytically-inactive non-essential Ypk1 substrate, yielded a readily detectable SDL phenotype.

Thus, using the protocol we devised, SDL may be a generally useful way to identify substrates and perhaps other binding partners of protein kinases, not just those directly connected to any output phenotype being measured.

Other genetic approaches have also been useful in identifying physiologically relevant targets of Ypk1. For example, a transposon insertion that suppressed the growth defect of a *ypk1-ts ypk2Δ* strain at an otherwise non-permissive temperature initially identifed Orm2 as a potential Ypk1 substrate (Roelants et al. 2002), a finding later corroborated by us (Roelants et al. 2011) and others (Berchtold et al. 2012; Liu et al. 2012; Niles et al. 2012; Sun et al. 2012). Similarly, Smp1, which we confirmed here is a likely Ypk1 substrate, was first identified as a potential Ypk1 target because it was isolated as a dosage suppressor of the temperature-sensitive phenotype of *ypk1-ts ypk2Δ* cells (Roelants et al. 2002). Smp1 is a transcription factor (de Nadal et al. 2003) that mediates iron toxicity (Lee et al. 2012a) and, similarly, Ypk1 is required for iron toxicity (Lee et al. 2012a). Thus, TORC2-Ypk1 signaling might be mechanistically coupled to iron metabolism by modulation of Smp1 transcriptional output.

Likewise, other situations where chemical genetics can be applied have proven useful in gleaning what aspects of cell function are controlled by a protein kinase. For example, mutagenesis of yeast Tor2 to confer susceptibility to a chemical inhibitor and thereby selectively inhibit TORC2 action has been achieved recently (Kliegman et al. 2013). This tool was combined with a coilection of deletion mutants to identify what processes, when eliminated, are especially deleterious to cell growth and survival when TORC2 action (and presumably Ypk1 activity) is limiting. This analysis suggested some connection between TORC2 action and the pentose-phosphate pathway (Kliegman et al. 2013), in keeping with the growth-promoting roles of both TORC1 and TORC2 and the demand for NADPH in many cellular anabolic reactions. Similarly, use of TOR inhibitors has implicated TORC2-Ypk1 signaling in regulation of actin filament formation that is somehow required for yeast cell survival in response to low levels of DNA damage (Shimada et al. 2013).

By contrast, the chemical genetic approach in our SDL method is quite different, in that it scores the deleterious effect arising from overexpression of a gene product (increased protein dosage) rather than from the total absence of a gene product, when activity of the kinase of interest is limited by inhibitor. Theoretically, under our conditions, we should also have been able to observe synthetic dosage rescue ("SDR"); however, we found no such examples. In any event, our method independently identified nearly all of the previously known *in vivo* substrates of Ypk1, as well as nearly a dozen genuine Ypk1 targets, including Lac1 and Lag1, that have only been pinpointed by our three-tiered method. Thus, our SDL screening technique provides a complementary approach for identifying substrates of a protein kinase above and beyond those accessible through genetic interactions between the kinase and single-gene deletions or other genetic schemes.

Many of the gene products identified by our screen are involved in processes that the TORC2-Ypk1 signaling axis is already known to regulate. For example, Ypk1 regulates glycerol-3-phosphate production via phosphorylation and inhibition of glycerol-3-phosphate dehydrogenase Gpd1 (Lee et al. 2012b). Interesting, a very likely Ypk1 target that met all of the criteria in our screen is Gpt2, sn-glycerol-3-phosphate 1-acyltransferase (Zheng and Zou 2001), an enzyme that esterifies glycerol-3-phosphate as the first step in glycerolipid formation. In this same regard, as another very likely Ypk1 target we also identified Fps1, a membrane channel (aquaglyceroporin) that regulates efflux of glycerol (a glycerol-3-phosphate-derived metabolite) (Luyten et al. 1995). These results strengthen the conclusion that TORC2-Ypk1 signaling is intimately involved in modulating the level of the precursor to both glycerophospholipids and the osmolyte glycerol (Lee et al. 2012b).

Ypk1 action has been implicated in regulation of both fluid phase and receptor-mediated endocytosis (deHart et al. 2002). In this regard, we identified as a very likely Ypk1 target an endocytic adaptor, the α-arrestin Rod1, which is necessary for ubiquitinylation-triggered internalization of nutrient permeases (Lin et al. 2008; Becuwe et al. 2012) and the pheromone

receptor Ste2 (Alvaro et al. 2014). Thus, as it does for PM lipids, TORC2-Ypk1 signaling may modulate PM protein composition via this α-arrestin, a possibility we are pursuing.

Ypk1 function has also been implicated in regulating production of reactive oxygen species (ROS) (Niles et al. 2014), but an as yet undefined mechanism. In our screen, we found Ysp2, a protein that regulates mitochondrial morphology and ROS levels (Sokolov et al. 2006), as a very likely Ypk1 substrate, possibly providing insight into the molecular basis of the connection between TORC2-Ypk1 signaling and ROS levels.

Similarly, several other prospects that were identified by our screen as very likely Ypk1 substrates remain to be validated. Such candidates include Muk1, a GEF for yeast Rab 5-type small GTPases (Vps21, Ypt52, and Ypt53) involved in vesicle-mediated Golgi body-to-endosome trafficking (Paulsel et al. 2013), suggesting that Ypk1 may also control switches that direct the flow of lipids. Muk1 is also intriguing for another potential reason. In *S. pombe*, a Rab 5-like GTPase (Ryh1) and its Muk1-like GEF were identified in a screen for TORC2 activators (Tatebe et al. 2010). Thus, if Ypk1-mediated phosphorylation inhibits Muk1 function, it could represent a negative feedback mechanism exerted on TORC2; conversely, if Ypk1-mediated phosphorylation stimulates Muk1 function, it could represent a mechanism for self-reinforcing maintenance of TORC2 activity and, thus, a high level of activated Ypk1. Clearly, by further investigating the physiological relevance of these and other remaining candidates much new biology may be learned. Indeed, several gene products of totally unknown function, such as Yhr097c and Ynr014w, as well as gene products (e.g., Atg21 and Pex31) not previous linked to either TORC2 or Ypk1, if validated, may provide new mechanistic insight into additional cellular processes regulated by TORC2-Ypk1 signaling.

Mechanism of phosphoregulation of ceramide synthase

As we have demonstrated here, TORC2-dependent Ypk1-mediated phosphorylation of Lac1 and Lag1 stimulates the function of the ceramide synthase complex. Consistent with our findings, a previous study found a consistent decrease in ceramide synthase activity in

602 microsomal fractions isolated from cells in which TORC2 had been inactivated (and thus Ypk1
603 activity was presumably reduced) (Aronova et al. 2008), although indirect effects of the loss of
604 TORC2 function on ceramide synthase activity could not be ruled out. Our findings make it clear
605 that the role of TORC2 is to promote the Ypk1-dependent phosphorylation of Lac1 and Lag1
606 subunits of this enzyme. However, the precise molecular mechanism by which this post-
607 translational modification stimulates this enzyme is still not completely clear. In this regard, it
608 has been shown that mammalian ceramide synthase activity increases upon heterodimerization
609 of different catalytic subunit isoforms (Laviad et al. 2012). However, as judged by co-immuno-
610 precipitation, we found no difference in the state of Lac1-Lag1 association between the wild-
611 type proteins and either our Lac1(S23A S24A) Lag1(S23A S24A) or Lac1(S23E S24E)
612 Lag1(S23E S24E) mutants (data not shown). As mentioned in Results, we found no difference
613 in the steady-state level of these same complexes or in their content of Lip1, a non-catalytic
614 component of the complexes also essential for ceramide synthase activity (Vallée and Riezman
615 2005). Thus, understanding of how phosphorylation of Ser23 and Ser24 in Lac1 and Lag1
616 stimulate ceramide synthase activity may require detail structural information, which will be
617 challenging to obtain for these polytopic integral membrane proteins.

618 ***TORC2-Ypk1 control of ceramide synthesis is conserved***

619 Although the enzymic steps that carry out sphingolipid biosynthesis have been largely
620 elucidated, much less was known, until recently, about regulation of these enzymes (Breslow
621 and Weissman 2010; Breslow 2013). The first insight came when it was demonstrated
622 (Roelants et al. 2011; Berchtold et al. 2012; Sun et al. 2012) that, in response to PM stresses,
623 including treatment with myriocin and aureobasidin A, TORC2-Ypk1 signaling is activated and
624 alleviates inhibition of the SPT complex by phosphorylating the negative regulatory proteins
625 Orm1 and Orm2 (Fig. 8). As a direct consequence, the rate of *de novo* production of the LCB
626 precursor to sphingolipids is increased. Although TORC2 signaling had been implicated in
627 promoting synthesis of ceramide, the product of LCB N-acylation (Aronova et al. 2008), it was

628 unknown whether that role was simply the result of TORC2-Ypk1-dependent stimulation of SPT
629 function and the resulting increase in LCB supply. As we demonstrated here, Ypk1-mediated
630 phosphorylation of Lac1 and Lag1 also increases in response to both myriocin and aureobasidin
631 A, suggesting that ceramide synthesis *per se*, and not simply general elevation of LCB levels, is
632 important for allowing the cells to cope with the effects of these antibiotics. Indeed, collectively,
633 the findings we describe here demonstrate unequivocally that, in addition to up-regulation of
634 SPT, TORC2-Ypk1 exerts direct control on the ceramide synthase step of the sphingolipid
635 biosynthetic pathway by phosphorylating and stimulating the function of the Lac1 and Lag1
636 subunits of the ceramide synthase complex. Moreover, as we also demonstrated, the ceramide
637 synthase reaction represents an important branch point in sphingolipid biosynthesis (Figs. 2B
638 and 8). LCBs produced by the SPT reaction can either be converted to ceramides or become
639 phosphorylated by LCB kinase Lcb4 (and its paralog Lcb5) to form LCBPs (Nagiec et al. 1998).
640 Accumulation of LCBPs has been shown to be toxic to yeast cell growth (Kim et al. 2000), as we
641 have also confirmed here, at least in large part because, as is now known, these metabolites
642 trigger inappropriate induction of autophagy (Zimmermann et al. 2013). Thus, the rate of
643 ceramide production must be properly adjusted to maintain the pool of LCBs and derived
644 LCBPs at a non-deleterious level, in agreement with evidence in yeast and other organisms that
645 ceramides and LCBPs generally play antagonist roles and must be maintained in the proper
646 dynamic balance (Kobayashi and Nagiec 2003; Spiegel and Milstien 2003; Kihara et al. 2007;
647 Dickson 2008; Breslow and Weissman 2010; Bikman and Summers 2011). Hence, the function
648 we have discovered and described here for TORC2-Ypk1 in stimulating ceramide synthase
649 promotes utilization of the increased LCB generated upon TORC2-Ypk1-mediated up-regulation
650 of SPT. This metabolic control has multiple clear-cut physiological benefits to the cell: (a)
651 directing flow in the sphingolipid pathway toward complex sphingolipids to populate the PM
652 barrier; (b) reduction of the level of potentially toxic LCBPs; and, (c) avoidance of inappropriate
653 induction of autophagy under nutrient-sufficient conditions (Fig. 8). Indeed, our results indicate

654 that a significant role for the coordination exerted by TORC2-Ypk1 between the level of SPT
655 activity and the level of ceramide synthase activity is to prevent metabolic "cross-talk" to the
656 autophagy pathway.

657 If this function of TORC2-Ypk1 signaling is important, then it should be conserved. Indeed,
658 alignments of the primary structures of Lac1 and Lag1 homologs predicted from sequenced
659 fungal genomes, from *Saccharomyces sensu stricto* species to the very distantly related
660 *Ustilago maydis*, nearly all contain a basophilic sequence that matches the Ypk1 phospho-
661 acceptor site consensus and is located, as in *S. cerevisiae* Lac1 and Lag1, in their N-terminal
662 cytosolic extensions, suggests that Ypk1-related protein kinases may regulate ceramide
663 synthase across essentially all fungal species. Consistent with this suggestion, a genetic
664 interaction between a Ypk1 homolog (YpkA) and a Lac1/Lag1-like ceramide synthase
665 component (BarA1) has been reported in *Aspergillus nidulans* (Colabardini et al. 2013).

666 There is also evidence that Orm1 and Orm2, when phosphorylated at unique sites by
667 protein kinase Npr1, promotes steps in the sphingolipid pathway that lead to more complex
668 sphingolipids (Shimobayashi et al. 2013). In contrast to Ypk1, which is activated by TORC2,
669 Npr1 is inhibited by TORC1 (MacGurn et al. 2011). Thus, this control mechanism will only be
670 exerted under conditions that inactivate TORC1, such as amino acid starvation (Loewith and
671 Hall 2011), a condition that presumably requires adjustment of both PM lipid and protein
672 composition to maximize the cell's ability to scavenge and assimilate nutrients. Under the same
673 condition, autophagy is induced because, like Npr1, TORC1 also negatively regulates the
674 autophagy-inducing protein kinase Atg1-Atg13 complex (Alers et al. 2014). Conversely, under
675 nutrient sufficient conditions, TORC1 is active, and phosphorylates and stimulates protein
676 kinase Sch9. Interestingly, Sch9 action should act in concert with TORC2-Ypk1 signaling to help
677 keep the levels of LCBs and LCBPs low and ceramides high. This is likely because Sch9
678 promotes transcriptional repression of genes (*YDC1* and *YPC1*) that encode ceramidases and
679 inhibits a phosphosphingolipid phospholipase C (Isc1) that hydrolyzes complex sphingolipids

680 (Swinnen et al. 2014). Such complex multi-component controls may be a general feature of
681 signaling modalities that interface with biosynthetic pathways that have intermediates, like
682 LCBPs, that are not inocuous, but are themselves bioactive metabolites.

683 ***Calcineurin negatively regulates ceramide synthase***

684 Prior studies had suggested that calcineurin negatively regulates sphingolipid production via
685 effects on the function of the ancillary TORC2 subunits, Slm1 and Slm2 (Bultynck et al. 2006;
686 Mulet et al. 2006; Tabuchi et al. 2006; Daquinag et al. 2007), although the molecular connection
687 between Slm1 and Slm2 and sphingolipid biosynthesis was unclear. Subsequently, it was
688 observed that, in cells lacking the regulatory subunit (Cnb1), there was an increase in C_{26}-
689 containing ceramides, suggesting that calcineurin somehow antagonizes TORC2-dependent
690 signaling (Aronova et al. 2008). We found that calcineurin negatively regulates ceramide
691 synthesis by directing the dephosphorylation of Lac1 and Lag1. This Ca^{2+}-activated calcineurin-
692 dependent dephosphorylation occurred even in cells expressing a TORC2-independent
693 constitutively-active Ypk1 allele. Moreover, we showed here that calcineurin does not affect
694 Pkh1- (and Pkh2-) mediated phosphorylation of the activation loop of Ypk1, and we
695 demonstrated previously that presence or absence of calcineurin does not alter TORC2-
696 mediated phosphorylation of Ypk1 or cause any substantial change in Ypk1 specific activity
697 (Roelants et al. 2011). Thus, direct down-modulation of either TORC2 or Ypk1 by calcineurin
698 cannot account for the negative regulation it exerts on sphingolipid biosynthesis. What our
699 findings now make clear is that calcineurin negatively regulates the sphingolipid pathway at the
700 level of ceramide synthesis, at least in large part, by direct dephosphorylation of the stimulatory
701 phosphorylations in the ceramide synthase subunits Lac1 and Lag1 that are installed by
702 TORC2-Ypk1 signaling. Calcineurin recognizes substrates via a docking motif (PxIxIT or
703 variants thereof), typically also accompanied quite a distance upstream by a secondary docking
704 site (LxVP) (Roy and Cyert 2009). However, these sites can be quite degenerate; for example,
705 the more hydrophobic variant PVIVIT is much more potent in recruiting calcineurin when it is

706 used to replace the native "PxIxIT" sequences in either the transcription factor Crz1 (PIISIQ)
707 (Roy et al. 2007) or the endocytic adaptor Aly1 (PILKIN) (O'Donnell et al. 2013). In both Lac1
708 and Lag1, there is a similar hydrophobic sequence located at the identical position in both
709 proteins (^{355}PIVFVL^{360}). Whether this or any other degenerate match represents a calcineurin-
710 binding site remains to be determined.

711 In conclusion, our screening approach has provided a number of new insights into how the
712 TORC2-Ypk1 axis modulates sphingolipid homeostasis and has uncovered a significant number
713 of candidate substrates that will very likely shed further light on other aspects of cellular function
714 that are regulated by TORC2-Ypk1 signaling.

715

716

717

Materials and Methods

Construction of yeast strains

All *S. cerevisiae* strains used in this study are listed in Table 2. Strains were constructed using standard yeast genetic manipulations (Burke et al. 2005). For all strains constructed, integration of the desired DNA fragment into the correct genomic loci was confirmed by PCR using an oligonucleotide complementary to the integrated DNA fragment and an oligonucleotide complementary to genomic sequence at least 150 bases away from the integration site.

Plasmids and recombinant DNA methods

All plasmids used in this study (except the library of P_{GAL1} based overexpression plasmids for synthetic dosage lethality (SDL) screening) are listed in Table 3. All plasmids were constructed and maintained in *E. coli* using standard laboratory methods (Green and Sambrook 2012). For SDL screening, the entire open reading frame of each predicted and known Ypk1 substrate was amplified by PCR from BY4741 genomic DNA and ligated into the multiple cloning site of YCpLG (*CEN*, P_{GAL1}, *LEU2*), generating a vector allowing galactose inducible overexpression of each substrate. All constructs generated in this study were confirmed by sequence analysis covering all promoter and coding regions in the construct.

Bioinformatic prediction of Ypk1 substrates

A Nx20 position weight matrix defining Ypk1 phosphoacceptor site specificity was made merging previously published data sets defining Ypk1 primary sequence specificity (Casamayor et al. 1999; Mok et al. 2010). This position weight matrix was then used with MOTIPS (Lam et al. 2010) to identify proteins with likely phosphorylated occurrences of this motif. Yeastmine (Balakrishnan et al. 2012) was used to identify all *S. cerevisiae* genes that showed genetic interactions with Ypk1, Ypk2, any component of the sphingolipid biosynthetic pathway or any component of known Ypk1 regulators (TORC2 and PP2A). Genes that showed significant growth phenotypes on myriocin, aureobasidin A and caspifungin (all compounds that cause severe growth phenotypes in *ypk1Δ* strains) were identified from the literature (Hillenmeyer et

al. 2008). Lastly, MOTIPS predicted Ypk1 phosphorylation sites were compared to Phosphogrid (Sadowski et al. 2013) to identify those sites known to be phosphorylated *in vivo*. To be considered a potential Ypk1 substrate in this study, a protein had to have a myriocin, aureobasidin or caspofungin phenotype or a Yeastmine identified genetic interaction and: (a) 4 or more MOTIPS predicted sites, (b) 3 sites with at least one above a MOTIPS likelihood score of 0.7 or a Phosphogrid identified site or (c) 1-2 sites with a MOTIPS likelihood score of 0.7 and a Phosphogrid identified site. We also considered for further analysis a limited number of proteins that did not meet these criteria, but which still contained Ypk1 motifs. These are indicated in Table 3.

Yeast growth assays and synthetic dosage lethality screening

For SDL screening, yAM135-A and BY4741 strains were both transformed with each SDL plasmid. Transformants were then cultured overnight in SC media containing 2% raffinose and 0.2% sucrose. 10 fold serial dilutions of overnight cultures starting from OD_{600} = 1.0 were then made in sterile water and spotted onto SC solid media with 2% galactose (to induce protein expression) or 2% dextrose (no protein expression). These plates also contained 1:1000 DMSO, 1 μM 3-MB-PP1 or 2 μM 3-MB-PP1 to inhibit to varying degrees Ypk1-as kinase activity in yAM135-A. Serially spotted cultures were allowed to grow in the dark at 30˚C for 3 days. Plates were then scanned on a flatbed scanner and growth phenotypes were assessed and scored.

For all SDL overexpression constructs that caused toxicity upon overexpression in WT BY4741 strains, we also performed Ypk1 dosage rescue growth assays. P_{MET25}-Ypk1 or P_{MET25}-Ypk1(K367A) (kinase dead) plasmids were co-transformed into BY4741 with the toxic SDL plasmid. Transformants were then cultured overnight in SC media containing 2% raffinose and 0.2% sucrose. 10 fold serial dilutions of overnight cultures starting from OD_{600} = 1.0 were then made in sterile water and spotted onto SC solid media with 2% galactose (to induce protein expression) or 2% dextrose (no protein expression), in the presence of absence of methionine

to drive Ypk1 overexpression. Serially spotted cultures were allowed to grow in the dark at 30˚C for 3 days. Plates were then scanned on a flatbed scanner and growth phenotypes were assessed to determine if Ypk1 overexpression could rescue toxicity of overexpression of the SDL protein.

For broth growth assays, log phase cultures growing in rich YP (Burke et al. 2005) media with 2% dextrose were diluted to OD_{600} = 0.1. 100 µL of each culture was placed in a well in a 96 well plate with vehicle or drug at the indicated concentration. Cultures were grown orbitally shaking at 30˚C in a Tecan Infinite M-1000 PRO plate reader (Tecan Systems Inc.) for 24 h. Absorbance measurements were taken every 15 min. Absorbance values were converted to OD_{600} values using a standard curve of absorbance values of cultures at known OD_{600} taken on the same plate reader.

Protein purification and* in vitro *Ypk1 kinase assay

To purify Ypk1-as kinase, pAX50 (2µ, P_{GAL1}-Ypk1-TAP, *URA3*) transformed yAM135-A yeasts were diluted to OD_{600} = 0.125 in 3L of SC 2% raffinose 0.2% sucrose and grown shaking at 30˚C to mid-exponential phase. Expression was induced for ~18 h by the addition of 2% galactose. Cells were harvested by centrifugation and frozen in liquid nitrogen. The cells were then lysed cryogenically using Mixer Mill MM301 (Retsch). The lysate was resuspended at 2 mL/g in TAP-B (50 mM Tris-Cl pH 7.5, 200 mM NaCl, 1.5 mM MgOAc, 1 mM DTT, 2 mM $NaVO_4$, 10 mM NaF, 10 mM Na-PPi, 10 mM β-glycerol phosphate, 1x cOmplete protease inhibitor (Roche)). The lysate was clarified by centrifugation at 15 kg for 20 min. Clarified lysate was then further centrifuged at 100 kg for 1 h and then brought to 0.15% NP-40 using 10% NP-40 detergent stock. Ypk1-as-TAP fusion was then affinity purified from the lysate using IgG-agarose resin (GE Healthcare). The resin was extensively washed with Protease 3C Buffer (50 mM Tris-Cl pH 7.5, 200 mM NaCl, 1.5 mM MgOAc, 1 mM DTT, 0.01% NP-40, 10% Glycerol, 2 mM $NaVO_4$, 10 mM NaF, 10 mM Na-PPi, 10 mM β-glycerol phosphate) and then resuspended in 1 mL Protease 3C Buffer. Ypk1-as was eluted by the addition of 80 U Prescission Protease

(GE Healthcare) for 5h at 4˚C. Protease 3C was removed by the addition of glutathione-agarose (GE Healthcare).

Putative Ypk1 substrates were expressed as N terminal GST fusions in BL21 *E. coli*. 1L cultures were grown at 37˚C to mid-exponential phase and then induced at room temperature for 4 h with 0.5 mM IPTG. Cells were harvested by centrifugation and the fusion proteins were purified by affinity chromatography using glutathione-agarose and standard procedures.

For kinase assays 0.25 µg of Ypk1-as kinase was incubated with purified GST-substrate fusion in Kinase Assay Buffer (50 mM Tris-Cl pH 7.5, 200 mM NaCl, 10 mM $MgCl_2$, 0.1 mM EDTA) with 2 µCi [γ-^{32}P]ATP at 30˚C in the presence of absence of 10 µM 3-MB-PP1 for 30 min. Reactions were terminated by the addition of SDS/PAGE sample buffer containing 6% SDS followed by boiling for 5 min. Labeled proteins were resolved by SDS/PAGE and analyzed Coomassie blue staining and autoradiography with Phosphorimager plates (Molecular Dynamics) on a Typhoon imaging system (GE Healthcare).

Preparation of cell extracts and immunoblotting

Cell extracts were made by alkaline lysis followed by trichloroacetic acid precipitation as previously described (Westfall et al. 2008). To resolve Lag1 and Lac1 phosphorylated species, 15 µL of TCA extract was resolved by SDS-PAGE (8% acrylamide, 35 µM Phos-tag (Wako Chemicals USA, Inc.), 35 µM $MnCl_2$ at 160 V). The gel was then transferred to nitrocellulose and incubated with primary antibody in Odyssey buffer (Licor Biosciences), washed, and incubated with IRDye680-conjugated anti-mouse IgG (Licor Biosciences) in Odyssey buffer with 0.1% Tween-20 and 0.02% SDS). Blots were imaged using an Odyssey infrared scanner (Licor Biosciences).

Primary antibodies and dilutions used in this study were: 1:1000 mouse anti-HA (Covance Inc.), 1:10000 mouse anti-FLAG (Sigma-Aldrich),1:500 mouse anti-GFP (Roche), 1:500 rabbit anti-pSGK (T256) (to recognize Ypk1 phosphorylated at T504) (Santa Cruz Biotechnology) and 1:10000 rabbit anti-Pgk1 (our laboratory).

For phosphatase treatment of cell extracts, TCA extracts were made as above and the precipitated proteins were solubilized in 100 µL Solubilization buffer (50 mM Tris-Cl pH 8.0, 150 mM NaCl, 2% β-mercaptoethanol, 2% SDS). These extracts were then diluted with 900 µL CIP Dilution buffer (50 mM Tris-Cl pH 8.0, 150 mM NaCl, 11.1 mM $MgCl_2$). 150 U calf intestinal phosphatase (New England Biolabs) was then added for 2 h at 37˚C. Proteins were then TCA precipitated again and resolved by SDS-PAGE as above.

Analysis of sphingolipid species

Complex sphingolipids were analyzed by thin layer chromatography. Cultures of strains in mid-exponential phase were adjusted to OD_{600} = 1.0 and 2 ml cultures were labeled with 100 µCi of [^{32}P] H_3PO_4 and cells allowed to grow for 3 h. Lipids were extracted and resolved as previously described (Hanson and Lester 1980; Momoi et al. 2004) with minor modifications. The cell pellet was washed twice with 2 ml water and treated with 5% trichloroacetic acid for 20 min on ice. Pellets were extracted twice with 0.75 ml of ethanol/water/diethyl-ether/pyridine/NH_4OH (15:15:5:1:0.018) at 60°C for 1 h. Glycerophospholipids in the extract were hydrolyzed by treating with 0.1 M monomethylamine at 50°C for 1 h after which the base was neutralized by addition of 12 µl of glacial acetic acid. Lipids were extracted with 1 ml chloroform, 0.5 ml methanol and phases separated with addition of 1 ml water. For some samples 1 ml of 4 N NaCl was used, in order to facilitate the separation of the aqueous and organic phases. The organic layer was dried under vacuum and resuspended in 50 µl of chloroform/methanol/water (16:16:5) and resolved on a silica gel TLC plate with chloform/methanol/4.2 N NH_4OH (9:7:2). Radioactivity on the TLC plate was visualized with a Phosphorimager screen and Typhoon imaging system.

LCBs and LCB-1Ps levels were monitored by liquid chromatography-mass spectrometry- Overnight cultures were adjusted to OD_{600} = 0.2 and allowed to grow to an OD_{600} = 1.0. Cell pellets from 10 ml of this culture equivalent to 10 OD_{600} units was used for analysis. C17-sphingosine (Avanti Polar Lipids), (5 nmol) was added to all samples as an internal standard.

Lipids were extracted as described above and the final dried lipid extract was dissolved in methanol/water/formic acid (79:20:1), centrifuged to remove insoluble material and an aliquot of this material was injected into the HPLC for analysis.

Lipid extracts were analyzed using an Agilent 1200 liquid chromatograph (LC; Santa Clara, CA) that was connected in-line with an LTQ Orbitrap XL mass spectrometer equipped with an electrospray ionization source (ESI; Thermo Fisher Scientific, Waltham, MA).

The LC was equipped with a C4 analytical column (Viva C4, 150 mm length × 1.0 mm inner diameter, 5 μm particles, 300 Å pores, Restek, Bellefonte, PA) and a 100 μL sample loop. Solvent A was 99.8% water/0.2% formic acid and solvent B was 99.8% methanol/0.2% formic acid (v/v). Solvents A and B both contained 5 mM ammonium formate. The sample injection volume was 85 μL (partial loop). The elution program consisted of isocratic flow at 30% B for 2 min, a linear gradient to 65% B over 0.1 min, a linear gradient to 100% B over 4.9 min, isocratic flow at 100% B for 4 min, a linear gradient to 30% B over 0.1 min, and isocratic flow at 30% B for 18.9 min, at a flow rate of 170 μL/min. The column and sample compartments were maintained at 40°C and 4°C, respectively. The injection needle was rinsed with a 1:1 methanol/water (v/v) solution after each injection.

The column exit was connected to the ESI probe of the mass spectrometer using PEEK tubing (0.005” inner diameter × 1/16” outer diameter, Agilent). Mass spectra were acquired in the positive ion mode over the range m/z = 250 to 1200 using the Orbitrap mass analyzer, in profile format, with a mass resolution setting of 100,000 (at m/z = 400, measured at full width at half-maximum peak height). In the data-dependent mode, the five most intense ions exceeding an intensity threshold of 30,000 counts were selected from each full-scan mass spectrum for tandem mass spectrometry (MS/MS) analysis using pulsed-Q dissociation (PQD). MS/MS spectra were acquired in the positive ion mode using the linear ion trap, in centroid format, with the following parameters: isolation width 3 m/z units, normalized collision energy 40%, and default charge state 1+. A parent mass list was used to preferentially select ions of interest for

874 targeted MS/MS analysis. To avoid the occurrence of redundant MS/MS measurements, real-
875 time dynamic exclusion was enabled to preclude re-selection of previously analyzed precursor
876 ions, using the following parameters: repeat count 2, repeat duration 30 s, exclusion list size
877 500, exclusion duration 180 s, and exclusion width 0.1 m/z unit. Data were analyzed using
878 Xcalibur software (version 2.0.7 SP1, Thermo) and LIPID MAPS Online Tools (Fahy et al.
879 2007).

880 Exact masses of precursor ions in positive ion ($M+H^+$) state obtained from LIPID MAPS
881 Online Tools were as follows- phytosphingosine- 318.3003, dihydrosphingosine-302.3053,
882 phytosphingosine-1 phosphate-398.2666 and dihydrosphingosine-1 phosphate- 382.2717. The
883 ions were further confirmed by tandem MS and identification of the fragments; product ions for
884 the phytosphingosine headgroup was 282.3 and dihydrosphigosine headgroup was 266.4.

885 **In vitro *ceramide synthase assay***

886 Yeast expressing 3xFLAG-Lag1 (wild-type and phospho-site mutations) were grown at 30°C to
887 mid-exponential phase and microsomes were prepared as described previously (Schorling et al.
888 2001) and resuspended in B88 buffer (20 mM HEPES-KOH pH 6.8, 150 mM KAc, 5 mM
889 MgOAc, and 250 mM sorbitol). Ceramide synthase was then immunopurified from these
890 microsomes using anti-FLAG agarose (Sigma) as described previously (Vallée and Riezman
891 2005). Prior to assembling ceramide synthase reactions, a small alioquot of each (15 µL)
892 immunoprecipitate was taken and proteins were resolved by SDS-PAGE and immunoblotted
893 with anti-FLAG to determine the relative amount of immunopurified ceramide synthase in each
894 reaction. Recovered ceramide levels for each reaction were normalized to the amount of
895 ceramide synthase determined by this procedure.

896 Ceramide synthesis reaction was assembled in B88 buffer with 5 mg/ml BSA, in a total
897 reaction volume of 0.1 ml containing, 47.5 µL anti-FLAG agarose immunoprecipitates, 50 µM
898 phytosphingosine and 0.1 mM of steroyl (C18)- CoA. Reactions were incubated at 30 °C for 1 h.
899 Reactions were terminated by addition of 0.4 ml methanol/$CHCl_3$ (2:1) and further extracted with

900 0.4 ml $CHCl_3$ and 0.4 ml water. The $CHCl_3$ phase was separated by centrifugation and removed
901 and dried under vacuum. The dried lipids resuspended in methanol/water/formic acid (79/20/1)
902 and an aliquot analyzed by LC-MS as described above. The product from the reaction, C18-
903 phytoceramide was identified by the exact mass of its precursor ion at 584.5612 and its product
904 ion upon fragmentation at 282.3. Additionally, authentic C18-phytoceramide (Matreya, LLC.)
905 standard was used to obtain a standard curve in order to establish that values from ceramide
906 synthase reaction were in the linear range of estimation.
907

Acknowledgements

This work was supported by an NIH Predoctoral Traineeship GM07232 and a Predoctoral Fellowship from the UC Systemwide Cancer Research Coordinating Committee (to A.M.) and by NIH R01 Research Grant GM21841 and Senior Investigator Award 11-0118 from the American Asthma Foundation (to J.T.). We thank Tony Iavarone in the QB3/Chemistry Mass Spectrometry Facility for expert assistance with the analysis of sphingolipids by mass spectrometry, Howard Riezman for the gift of the FLAG-Lip1 construct, Jonathan Weissman, Martha Cyert, Benjamin Turk, Daniel Klionsky, and Hidetoshi Iida for other strains or plasmids, Jeffrey Liu and Brian Ting for technical assistance, and other members of the Thorner Lab for various reagents, plasmids, and many helpful discussions.

References

Alers S, Wesselborg S, Stork B. 2014. ATG13: Just a companion, or an executor of the autophagic program? *Autophagy* **10**: 944-956.

Alvaro CG, O'Donnell AF, Prosser DC, Augustine AA, Goldman A, Brodsky JL, Cyert MS, Wendland B, Thorner J. 2014. Specific alpha-arrestins negatively regulate *Saccharomyces cerevisiae* pheromone response by down-modulating the G-protein coupled receptor Ste2. *Mol Cell Biol* **34**: 2660-2681.

Ansell R, Granath K, Hohmann S, Thevelein JM, Adler L. 1997. The two isoenzymes for yeast NAD+-dependent glycerol 3-phosphate dehydrogenase encoded by GPD1 and GPD2 have distinct roles in osmoadaptation and redox regulation. *EMBO J* **16**: 2179-2187.

Aronova S, Wedaman K, Aronov PA, Fontes K, Ramos K, Hammock BD, Powers T. 2008. Regulation of ceramide biosynthesis by TOR complex 2. *Cell Metab* **7**: 148-158.

Balakrishnan R, Park J, Karra K, Hitz BC, Binkley G, Hong EL, Sullivan J, Micklem G, Cherry JM. 2012. YeastMine--an integrated data warehouse for Saccharomyces cerevisiae data as a multipurpose tool-kit. *Database (Oxford)* **2012**: bar062.

Bardwell L, Cook JG, Zhu-Shimoni JX, Voora D, Thorner J. 1998. Differential regulation of transcription: repression by unactivated mitogen-activated protein kinase Kss1 requires the Dig1 and Dig2 proteins. *Proc Natl Acad Sci U S A* **95**: 15400-15405.

Barz WP, Walter P. 1999. Two endoplasmic reticulum (ER) membrane proteins that facilitate ER-to-Golgi transport of glycosylphosphatidylinositol-anchored proteins. *Mol Biol Cell* **10**: 1043-1059.

Becuwe M, N. V, Lara D, Gomes-Rezende J, Soares-Cunha C, Casal M, Haguenauer-Tsapis R, Vincent O, Paiva S, Léon S. 2012. A molecular switch on an arrestin-like protein relays glucose signaling to transporter endocytosis. *J Cell Biol* **196**: 247-259.

Beeler T, Bacikova D, Gable K, Hopkins L, Johnson C, Slife H, Dunn T. 1998. The *Saccharomyces cerevisiae* TSC10/YBR265w gene encoding 3-ketosphinganine reductase is identified in a screen for temperature-sensitive suppressors of the Ca^{2+}-sensitive csg2Δ mutant. *J Biol Chem* **273**: 30688-30694.

Berchtold D, Piccolis M, Chiaruttini N, Riezman I, Riezman H, Roux A, Walther TC, Loewith R. 2012. Plasma membrane stress induces relocalization of Slm proteins and activation of TORC2 to promote sphingolipid synthesis. *Nat Cell Biol* **14**: 542-547.

Bikman BT, Summers SA. 2011. Ceramides as modulators of cellular and whole-body metabolism. *J Clin Invest* **121**: 4222-4230.

Breslow DK. 2013. Sphingolipid homeostasis in the endoplasmic reticulum and beyond. *Cold Spring Harb Perspect Biol* **5**: a013326.013321-013316.

Breslow DK, Weissman JS. 2010. Membranes in balance: mechanisms of sphingolipid homeostasis. *Mol Cell* **40**: 267-279.

Bultynck G, Heath VL, Majeed AP, Galan JM, Haguenauer-Tsapis R, Cyert MS. 2006. Slm1 and slm2 are novel substrates of the calcineurin phosphatase required for heat stress-induced endocytosis of the yeast uracil permease. *Mol Cell Biol* **26**: 4729-4745.

Burkard ME, Randall CL, Larochelle S, Zhang C, K.M. S, Fisher RP, Jallepalli PV. 2007. Chemical genetics reveals the requirement for Polo-like kinase 1 activity in positioning RhoA and triggering cytokinesis in human cells. *Proc Nat Acad Sci USA* **104**: 4383-4388.

Burke D, Amberg D, Strathern J. 2005. *Methods in Yeast Genetics: A Cold Spring Harbor Laboratory Course Manual*. Cold Spring Harbor Laboratory Press.

Byrne KP, Wolfe KH. 2005. The Yeast Gene Order Browser: combining curated homology and syntenic context reveals gene fate in polyploid species. *Genome Res* **15**: 1456-1461.

965 Casamayor A, Torrance PD, Kobayashi T, Thorner J, Alessi DR. 1999. Functional counterparts of
966 mammalian protein kinases PDK1 and SGK in budding yeast. *Curr Biol* **9**: 186-197.
967 Chen PW, Fonseca LL, Hannun YA, Voit EO. 2013. Coordination of rapid sphingolipid responses to heat
968 stress in yeast. *PLoS Comput Biol* **9**: e1003078.
969 Colabardini AC, Brown NA, Savoldi M, Goldman MH, Goldman GH. 2013. Functional characterization of
970 Aspergillus nidulans ypkA, a homologue of the mammalian kinase SGK. *PLoS One* **8**: e57630.
971 Cowart LA, Okamoto Y, Pinto FR, Gandy JL, Almeida JS, Hannun YA. 2003. Roles for sphingolipid
972 biosynthesis in mediation of specific programs of the heat stress response determined through
973 gene expression profiling. *J Biol Chem* **278**: 30328-30338.
974 Daquinag A, Fadri M, Jung SY, Qin J, Kunz J. 2007. The yeast PH domain proteins Slm1 and Slm2 are
975 targets of sphingolipid signaling during the response to heat stress. *Mol Cell Biol* **27**: 633-650.
976 de Nadal E, Casadomé L, Posas F. 2003. Targeting the MEF2-like transcription factor Smp1 by the stress-
977 activated Hog1 mitogen-activated protein kinase. *Mol Cell Biol* **23**: 229-237.
978 deHart AK, Schnell JD, Allen DA, Hicke L. 2002. The conserved Pkh-Ypk kinase cascade is required for
979 endocytosis in yeast. *J Cell Biol* **156**: 241-248.
980 Dickson RC. 2008. Thematic review series: sphingolipids. New insights into sphingolipid metabolism and
981 function in budding yeast. *J Lipid Res* **49**: 909-921.
982 Divito CB, Amara SG. 2009. Close encounters of the oily kind: regulation of transporters by lipids. *Mol*
983 *Interv* **9**: 252-262.
984 Fahy E, Sud M, Cotter D, Subramaniam S. 2007. LIPID MAPS online tools for lipid research. *Nucleic Acids*
985 *Res* **35**: W606-612.
986 Green MR, Sambrook J. 2012. *Molecular cloning : a laboratory manual*. Cold Spring Harbor Laboratory
987 Press, Cold Spring Harbor, N.Y.
988 Groves JT, Kuriyan J. 2010. Molecular mechanisms in signal transduction at the membrane. *Nat Struct*
989 *Mol Biol* **17**: 659-665. .
990 Gwinn DM, Shackelford DB, Egan DF, Mihaylova MM, Mery A, Vasquez DS, Turk BE, Shaw RJ. 2008.
991 AMPK phosphorylation of raptor mediates a metabolic checkpoint. *Mol Cell* **30**: 214-226.
992 Hanson BA, Lester RL. 1980. The extraction of inositol-containing phospholipids and phosphatidylcholine
993 from Saccharomyces cerevisiae and Neurospora crassa. *J Lipid Res* **21**: 309-315.
994 Heidler SA, Radding JA. 1995. The AUR1 gene in *Saccharomyces cerevisiae* encodes dominant resistance
995 to the antifungal agent aureobasidin A (LY295337). *Antimicrob Agents Chemother* **39**: 2765-
996 2769.
997 Hillenmeyer ME, Fung E, Wildenhain J, Pierce SE, Hoon S, Lee W, Proctor M, St Onge RP, Tyers M, Koller
998 D et al. 2008. The chemical genomic portrait of yeast: uncovering a phenotype for all genes.
999 *Science* **320**: 362-365.
1000 Holt LJ, Hutti JE, Cantley LC, Morgan DO. 2007. Evolution of Ime2 phosphorylation sites on Cdk1
1001 substrates provides a mechanism to limit the effects of the phosphatase Cdc14 in meiosis. *Mol*
1002 *Cell* **25**: 689-702.
1003 Hutti JE, Shen RR, Abbott DW, Zhou AY, Sprott KM, Asara JM, Hahn WC, Cantley LC. 2009.
1004 Phosphorylation of the tumor suppressor CYLD by the breast cancer oncogene IKKepsilon
1005 promotes cell transformation. *Mol Cell* **34**: 461-472.
1006 Iida K, Teng J, Tada T, Saka A, Tamai M, Izumi-Nakaseko H, Adachi-Akahane S, Iida H. 2007. Essential,
1007 completely conserved glycine residue in the domain III S2-S3 linker of voltage-gated calcium
1008 channel alpha1 subunits in yeast and mammals. *J Biol Chem* **282**: 25659-25667.
1009 Ikeda K, Morigasaki S, Tatebe H, Tamanoi F, Shiozaki K. 2008. Fission yeast TOR complex 2 activates the
1010 AGC-family Gad8 kinase essential for stress resistance and cell cycle control. *Cell Cycle* **7**: 358-
1011 364.

1012 Jacinto E, Facchinetti V, Liu D, Soto N, Wei S, Jung SY, Huang Q, J. Q, Su B. 2006. SIN1/MIP1 maintains
1013 rictor-mTOR complex integrity and regulates Akt phosphorylation and substrate specificity. *Cell*
1014 **127**: 125-137.
1015 Jenkins GM, Richards A, Wahl T, Mao C, Obeid L, Hannun Y. 1997. Involvement of yeast sphingolipids in
1016 the heat stress response of *Saccharomyces cerevisiae*. *J Biol Chem* **272**: 32566-32572.
1017 Jiang JC, Kirchman PA, Zagulski M, Hunt J, Jazwinski SM. 1998. Homologs of the yeast longevity gene
1018 LAG1 in Caenorhabditis elegans and human. *Genome Res* **8**: 1259-1272.
1019 Kageyama-Yahara N, Riezman H. 2006. Transmembrane topology of ceramide synthase in yeast.
1020 *Biochem J* **398**: 585-593.
1021 Kamada Y, Fujioka Y, Suzuki NN, Inagaki F, Wullschleger S, Loewith R, Hall MN, Ohsumi Y. 2005. Tor2
1022 directly phosphorylates the AGC kinase Ypk2 to regulate actin polarization. *Mol Cell Biol* **25**:
1023 7239-7248.
1024 Kataoka S, Furuita K, Hattori Y, Kobayashi N, Ikegami T, Shiozaki K, Fujiwara T, Kojima C. 2014. ^{1}H, ^{15}N
1025 and ^{13}C resonance assignments of the conserved region in the middle domain of *S. pombe* Sin1
1026 protein. *Biomol NMR Assign* [Epub ahead of print, 8 March 2014].
1027 Kihara A, Mitsutake S, Mizutani Y, Igarashi Y. 2007. Metabolism and biological functions of two
1028 phosphorylated sphingolipids, sphingosine 1-phosphate and ceramide 1-phosphate. *Prog Lipid*
1029 *Res* **46**: 126-144.
1030 Kim S, Fyrst H, Saba J. 2000. Accumulation of phosphorylated sphingoid long chain bases results in cell
1031 growth inhibition in Saccharomyces cerevisiae. *Genetics* **156**: 1519-1529.
1032 Kinoshita E, Kinoshita-Kikuta E, Koike T. 2009. Separation and detection of large phospho-proteins using
1033 Phos-tag SDS-PAGE. *Nat Protoc* **4**: 1513–1521.
1034 Kliegman JI, Fiedler D, Ryan CJ, Xu YF, Su XY, Thomas D, Caccese MC, Cheng A, Shales M, Rabinowitz JD
1035 et al. 2013. Chemical genetics of rapamycin-insensitive TORC2 in S. cerevisiae. *Cell Rep* **5**: 1725-
1036 1736.
1037 Kobayashi SD, Nagiec MM. 2003. Ceramide/long-chain base phosphate rheostat in Saccharomyces
1038 cerevisiae: regulation of ceramide synthesis by Elo3p and Cka2p. *Eukaryot Cell* **2**: 284-294.
1039 Lam HY, Kim PM, Mok J, Tonikian R, Sidhu SS, Turk BE, Snyder M, Gerstein MB. 2010. MOTIPS:
1040 automated motif analysis for predicting targets of modular protein domains. *BMC*
1041 *Bioinformatics* **11**: 243.
1042 Laviad EL, Kelly S, Merrill AH, Futerman AH. 2012. Modulation of ceramide synthase activity via
1043 dimerization. *J Biol Chem* **287**: 21025-21033.
1044 Lee YJ, Huang X, Kropat J, Henras A, Merchant SS, Dickson RC, Chanfreau GF. 2012a. Sphingolipid
1045 signaling mediates iron toxicity. *Cell Metab* **16**: 90-96.
1046 Lee YJ, Jeschke GR, Roelants FM, Thorner J, Turk BE. 2012b. Reciprocal phosphorylation of yeast
1047 glycerol-3-phosphate dehydrogenases in adaptation to distinct types of stress. *Mol Cell Biol* **32**:
1048 4705-4717.
1049 Liao HC, Chen MY. 2012. Target of rapamycin complex 2 signals to downstream effector yeast protein
1050 kinase 2 (Ypk2) through adheres-voraciously-to-target-of-rapamycin-2 protein 1 (Avo1) in
1051 *Saccharomyces cerevisiae*. *J Biol Chem* **287**: 6089-6099.
1052 Lin CH, MacGurn JA, Chu T, Stefan CJ, Emr SD. 2008. Arrestin-related ubiquitin-ligase adaptors regulate
1053 endocytosis and protein turnover at the cell surface. *Cell* **135**: 714-725.
1054 Lin D, Yin X, Wang X, Zhou P, Guo FB. 2013. Re-annotation of protein-coding genes in the genome of
1055 *Saccharomyces cerevisiae* based on support vector machines. *PLoS One* **8**: e64477.64471-64476.
1056 Linding R, Jensen LJ, Ostheimer GJ, van Vugt MA, Jørgensen C, Miron IM, Diella F, Colwill K, Taylor L,
1057 Elder K et al. 2007. Systematic discovery of in vivo phosphorylation networks. *Cell* **129**: 1415-
1058 1426.

1059 Liu M, Huang C, Polu SR, Schneiter R, Chang A. 2012. Regulation of sphingolipid synthesis through Orm1
1060 and Orm2 in yeast. *J Cell Sci* **125**: 2428-2435.
1061 Liu P, Gan W, Inuzuka H, Lazorchak AS, Gao D, Arojo O, Liu D, Wan L, Zhai B, Yu Y et al. 2013. Sin1
1062 phosphorylation impairs mTORC2 complex integrity and inhibits downstream Akt signalling to
1063 suppress tumorigenesis. *Nat Cell Biol* **15**: 1340-1350.
1064 Loewith R, Hall MN. 2011. Target of rapamycin (TOR) in nutrient signaling and growth control. *Genetics*
1065 **189**: 1177-1201.
1066 Lu M, Wang J, Ives HE, Pearce D. 2011. mSIN1 protein mediates SGK1 protein interaction with mTORC2
1067 protein complex and is required for selective activation of the epithelial sodium channel. *J Biol*
1068 *Chem* **286**: 30647-30654. .
1069 Luyten K, Albertyn J, Skibbe WF, Prior BA, Ramos J, Thevelein JM, Hohmann S. 1995. Fps1, a yeast
1070 member of the MIP family of channel proteins, is a facilitator for glycerol uptake and efflux and
1071 is inactive under osmotic stress. *EMBO J* **14**: 1360-1371.
1072 MacGurn JA, Hsu PC, Smolka MB, Emr SD. 2011. TORC1 regulates endocytosis via Npr1-mediated
1073 phosphoinhibition of a ubiquitin ligase adaptor. *Cell* **147**.
1074 Mah AS, Elia AE, Devgan G, Ptacek J, Schutkowski M, Snyder M, Yaffe MB, Deshaies RJ. 2005. Substrate
1075 specificity analysis of protein kinase complex Dbf2-Mob1 by peptide library and proteome array
1076 screening. *BMC Biochem* **6**: 22.
1077 Mandala SM, Thornton R, Tu Z, Kurtz MB, Nickels J, Broach J, Menzeleev R, Spiegel S. 1998. Sphingoid
1078 base 1-phosphate phosphatase: a key regulator of sphingolipid metabolism and stress response.
1079 *Proc Natl Acad Sci, USA* **95**: 150-155.
1080 Manning BD, Tee AR, Logsdon MN, Blenis J, Cantley LC. 2002. Identification of the tuberous sclerosis
1081 complex-2 tumor suppressor gene product tuberin as a target of the phosphoinositide 3-
1082 kinase/akt pathway. *Mol Cell* **10**: 151-162.
1083 Mok J, Kim PM, Lam HY, Piccirillo S, Zhou X, Jeschke GR, Sheridan DL, Parker SA, Desai V, Jwa M et al.
1084 2010. Deciphering protein kinase specificity through large-scale analysis of yeast
1085 phosphorylation site motifs. *Sci Signal* **3**: ra12.
1086 Momoi M, Tanoue D, Sun Y, Takematsu H, Suzuki Y, Suzuki M, Suzuki A, Fujita T, Kozutsumi Y. 2004. SLI1
1087 (YGR212W) is a major gene conferring resistance to the sphingolipid biosynthesis inhibitor ISP-1,
1088 and encodes an ISP-1 N-acetyltransferase in yeast. *Biochem J* **381**: 321-328.
1089 Mora A, Komander D, van Aalten DM, Alessi DR. 2004. PDK1, the master regulator of AGC kinase signal
1090 transduction. *Semin Cell Dev Biol* **15**: 161-170.
1091 Mulet JM, Martin DE, Loewith R, Hall MN. 2006. Mutual antagonism of target of rapamycin and
1092 calcineurin signaling. *J Biol Chem* **281**: 33000-33007.
1093 Nagiec MM, Nagiec EE, Baltisberger JA, Wells G, Lester RL, Dickson RC. 1997. Sphingolipid synthesis as a
1094 target for antifungal drugs. Complementation of the inositol phosphorylceramide synthase
1095 defect in a mutant strain of *Saccharomyces cerevisiae* by the *AUR1* gene. *J Biol Chem* 9809-9817.
1096 Nagiec MM, Skrzypek M, Nagiec EE, Lester RL, Dickson RC. 1998. The LCB4 (YOR171c) and LCB5
1097 (YLR260w) genes of Saccharomyces encode sphingoid long chain base kinases. *J Biol Chem* **273**:
1098 19437-19442.
1099 Niles BJ, Joslin AC, Fresques T, Powers T. 2014. TOR Complex 2-Ypk1 Signaling Maintains Sphingolipid
1100 Homeostasis by Sensing and Regulating ROS Accumulation. *Cell Rep*.
1101 Niles BJ, Mogri H, Hill A, Vlahakis A, Powers T. 2012. Plasma membrane recruitment and activation of
1102 the AGC kinase Ypk1 is mediated by target of rapamycin complex 2 (TORC2) and its effector
1103 proteins Slm1 and Slm2. *Proc Natl Acad Sci U S A* **109**: 1536-1541.
1104 Niles BJ, Powers T. 2012. Plasma membrane proteins Slm1 and Slm2 mediate activation of the AGC
1105 kinase Ypk1 by TORC2 and sphingolipids in S. cerevisiae. *Cell Cycle* **11**: 3745-3749.

O'Donnell AF, Huang L, Thorner J, Cyert MS. 2013. A calcineurin-dependent switch controls the trafficking function of alpha-arrestin Aly1/Art6. *J Biol Chem* **288**: 24063–24080. .

Papinski D, Kraft C. 2014. Atg1 kinase organizes autophagosome formation by phosphorylating Atg9. *Autophagy* **10**: [Epub ahead of print, 29 April 2014].

Paulsel AL, Merz AJ, Nickerson DP. 2013. Vps9 family protein Muk1 is the second Rab5 guanosine nucleotide exchange factor in budding yeast. *J Biol Chem* **288**: 18162-18171.

Pearce L, Komander D, Alessi DR. 2010. The nuts and bolts of AGC protein kinases. *Nat Rev Mol Cell Biol* **11**: 9-22.

Platta HW, Stenmark H. 2011. Endocytosis and signaling. *Curr Opin Cell Biol* **23**: 393-403.

Rennefahrt UE, Deacon SW, Parker SA, Devarajan K, Beeser A, Chernoff J, Knapp S, Turk BE, Peterson JR. 2007. Specificity profiling of Pak kinases allows identification of novel phosphorylation sites. *J Biol Chem* **282**: 15667-15678.

Roelants FM, Baltz AG, Trott AE, Fereres S, Thorner J. 2010. A protein kinase network regulates the function of aminophospholipid flippases. *Proc Natl Acad Sci USA* **107**: 34-39.

Roelants FM, Breslow DK, Muir A, Weissman JS, Thorner J. 2011. Protein kinase Ypk1 phosphorylates regulatory proteins Orm1 and Orm2 to control sphingolipid homeostasis in *Saccharomyces cerevisiae*. *Proc Natl Acad Sci USA* **108**: 19222-19227.

Roelants FM, Torrance PD, Bezman N, Thorner J. 2002. Pkh1 and Pkh2 differentially phosphorylate and activate Ypk1 and Ykr2 and define protein kinase modules required for maintenance of cell wall integrity. *Mol Biol Cell* **13**: 3005-3028.

Roelants FM, Torrance PD, Thorner J. 2004. Differential roles of PDK1- and PDK2-phosphorylation sites in the yeast AGC kinases Ypk1, Pkc1 and Sch9. *Microbiology* **150**: 3289-3304.

Roy J, Cyert MS. 2009. Cracking the phosphatase code: docking interactions determine substrate specificity. *Sci Signal* **2**: re9.1-7.

Roy J, Li H, Hogan PG, Cyert MS. 2007. A conserved docking site modulates substrate affinity for calcineurin, signaling output, and in vivo function. *Mol Cell* **25**: 889-901.

Sachs JN, Engelman DM. 2006. Introduction to the membrane protein reviews: the interplay of structure, dynamics, and environment in membrane protein function. *Annu Rev Biochem* **75**: 707-712.

Sadowski I, Breitkreutz BJ, Stark C, Su TC, Dahabieh M, Raithatha S, Bernhard W, Oughtred R, Dolinski K, Barreto K et al. 2013. The PhosphoGRID Saccharomyces cerevisiae protein phosphorylation site database: version 2.0 update. *Database (Oxford)* **2013**: bat026.

Schorling S, Vallée B, Barz WP, Riezman H, Oesterhelt D. 2001. Lag1p and Lac1p are essential for the acyl-CoA-dependent ceramide synthase reaction in *Saccharomyces cerevisiae*. *Mol Biol Cell* **12**: 3417-3427.

Sharifpoor S, van Dyk D, Costanzo M, Baryshnikova A, Friesen H, Douglas AC, Youn JY, VanderSluis B, Myers CL, Papp B et al. 2012. Functional wiring of the yeast kinome revealed by global analysis of genetic network motifs. *Genome Res* **22**: 791-801.

Shimada K, Filipuzzi I, Stahl M, Helliwell SB, Studer C, Hoepfner D, Seeber A, Loewith R, Movva NR, Gasser SM. 2013. TORC2 signaling pathway guarantees genome stability in the face of DNA strand breaks. *Mol Cell* **51**: 829-839.

Shimobayashi M, Oppliger W, Moes S, Jenö P, Hall MN. 2013. TORC1-regulated protein kinase Npr1 phosphorylates Orm to stimulate complex sphingolipid synthesis. *Mol Biol Cell* **24**: 870-881.

Sikorski RS, Hieter P. 1989. A system of shuttle vectors and yeast host strains designed for efficient manipulation of DNA in Saccharomyces cerevisiae. *Genetics* **122**: 19-27.

Simons K, Sampaio JL. 2011. Membrane organization and lipid rafts. *Cold Spring Harb Perspect Biol* **3**: a004697.004691-004617.

Sokolov S, Knorre D, Smirnova E, Markova O, Pozniakovsky A, Skulachev V, Severin F. 2006. Ysp2 mediates death of yeast induced by amiodarone or intracellular acidification. *Biochim Biophys Acta* **1757**: 1366-1370.

Sopko R, Huang D, Preston N, Chua G, Papp B, Kafadar K, Snyder M, Oliver SG, Cyert M, Hughes TR et al. 2006. Mapping pathways and phenotypes by systematic gene overexpression. *Mol Cell* **21**: 319-330.

Spiegel S, Milstien S. 2003. Sphingosine-1-phosphate: an enigmatic signalling lipid. *Nat Rev Mol Cell Biol* **4**: 397-407.

Stathopoulos-Gerontides A, Guo JJ, Cyert MS. 1999. Yeast calcineurin regulates nuclear localization of the Crz1p transcription factor through dephosphorylation. *Genes Dev* **13**: 798-803.

Sun Y, Miao Y, Yamane Y, Zhang C, Shokat KM, Takematsu H, Kozutsumi Y, Drubin DG. 2012. Orm protein phosphoregulation mediates transient sphingolipid biosynthesis response to heat stress via the Pkh-Ypk and Cdc55-PP2A pathways. *Mol Biol Cell* **23**: 2388-2398.

Swinnen E, Wilms T, Idkowiak-Baldys J, Smets B, De Snijder P, Accardo S, Ghillebert R, Thevissen K, Cammue B, De Vos D et al. 2014. The protein kinase Sch9 is a key regulator of sphingolipid metabolism in *Saccharomyces cerevisiae. Mol Biol Cell* **25**: 196-211.

Tabuchi M, Audhya A, Parsons AB, Boone C, Emr SD. 2006. The phosphatidylinositol 4,5-biphosphate and TORC2 binding proteins Slm1 and Slm2 function in sphingolipid regulation. *Mol Cell Biol* **26**: 5861-5875.

Tatebe H, Morigasaki S, Murayama S, Zeng CT, Shiozaki K. 2010. Rab-family GTPase regulates TOR complex 2 signaling in fission yeast. *Curr Biol* **20**: 1975-1982.

Vallée B, Riezman H. 2005. Lip1p: a novel subunit of acyl-CoA ceramide synthase. *EMBO J* **24**: 730-741.

Westfall PJ, Patterson JC, Chen RE, Thorner J. 2008. Stress resistance and signal fidelity independent of nuclear MAPK function. *Proc Natl Acad Sci U S A* **105**: 12212-12217.

Yaffe MB, Leparc GG, Lai J, Obata T, Volinia S, Cantley LC. 2001. A motif-based profile scanning approach for genome-wide prediction of signaling pathways. *Nat Biotechnol* **19**: 348-353.

Yang Q, Inoki K, Ikenoue T, Guan KL. 2006. Identification of Sin1 as an essential TORC2 component required for complex formation and kinase activity. . *Genes Dev* **20**: 2820-2832.

Zheng Z, Zou J. 2001. The initial step of the glycerolipid pathway: identification of glycerol 3-phosphate/dihydroxyacetone phosphate dual substrate acyltransferases in Saccharomyces cerevisiae. *J Biol Chem* **276**: 41710-41716.

Zimmermann C, Santos A, Gable K, Epstein S, Gururaj C, Chymkowitch P, Pultz D, Rødkær SV, Clay L, Bjørås M et al. 2013. TORC1 inhibits GSK3-mediated Elo2 phosphorylation to regulate very long chain fatty acid synthesis and autophagy. *Cell Rep* **5**: 1036-1046.

Table 1. Known Ypk1 substrates and potential substrates predicted by MOTIPS listed under GO Slim terms.[a]

Gene	MOTIPS Sites	Chemical Sensitivity/YeastMine Interaction(s)	SDL Score	Ypk1 Dosage Rescue	*In vitro* substrate
Known Ypk1 Substrates					
GPD1/YDL022W*	24[P]	YeastMine	+++	N/A	+
FPK1/YNR047W	37, 200, 244, 436, 481	YeastMine	+	N/A	+
FPK1(D621A) [Kinase-dead mutant]	37, 200, 244, 436, 481	YeastMine	++	N/A	+
ORM1/YGR038W	52, 53	YeastMine	+++	N/A	+
ORM2/YLR350W	47, 48	YeastMine	++++	N/A	+
Cytoskeleton Organization					
AVO1/YOL078W	552[P],597,1078	YeastMine	-	N/A	N/A
AVO2/YMR068W	273[P], 305, 407	YeastMine	-	N/A	N/A
BEM2/YER155C	83, 168, 1810, 1813	Myr, YeastMine	-	N/A	N/A
BNI1/YNL271C	119, 1138[P], 1533	AbA, Casp, YeastMine	-	N/A	N/A
CDH1/YGL003C	51, 195, 213[P]	AbA, YeastMine	TOXIC	-	N/A
ENT1/YDL161W	160[P]	YeastMine	-	N/A	N/A
GIC2/YDR309C	90, 312, 345[P]	Myr, AbA	-	N/A	N/A

LSB3/YFR024C-A	262[P]	YeastMine	-	N/A	N/A
PAL1/YDR348C	49[P], 391, 436	AbA, Casp	++++	N/A	-
SLA1/YBL007C	445, 447[P], 449[P], 477	YeastMine	-	N/A	N/A
TSC11/YER093C	19[P], 97, 188	YeastMine	N/A	N/A	N/A
YHR097C	58, 288[P], 294[P]	Myr	+++	N/A	+/-
YSC84/YHR016C	274, 374[P]	Myr, YeastMine	-	N/A	N/A

Biological Process

Unknown

COM2/YER130C	251, 370, 380	Myr, YeastMine	-	N/A	N/A
ECM3/YOR092W*	312, 350	Myr, AbA, YeastMine	-	N/A	N/A
ICS2/YBR157C	14, 95, 136, 172[P]	Myr	-	N/A	N/A
JIP4/YDR475C	348, 352, 592, 649	Myr, AbA	N/A	N/A	N/A
KKQ8/YKL168C	83, 113, 144, 146, 212, 293	YeastMine	-	N/A	N/A
RTS3/YGR161C*	30, 238[P]	YeastMine	-	N/A	N/A
SEG1/YMR086W	56, 118[P], 217, 634, 752[P]	Myr	+	N/A	N/A
YDR186C	334[P], 540[P], 542[P], 620, 715[P]	YeastMine	-	N/A	N/A
YHR080C	401, 513, 667	YeastMine	-	N/A	N/A

YNR014W	54, 115, 156, 197	YeastMine	+++	N/A	+
YPK3/YBR028C	72, 73, 90[P]	Myr, Casp	-	N/A	N/A

Transcription from RNA

Polymerase II Promoter

EPL1/YFL024C	24, 28, 61	YeastMine	-	N/A	N/A
FKH1/YIL131C	404	Myr, YeastMine	TOXIC	-	-
GAL11/YOL051W	1003[P]	Myr, YeastMine	-	N/A	N/A
HCM1/YCR065W*	80	AbA, YeastMine	-	N/A	N/A
HOT1/YMR172W*	387, 520, 586	Myr	-	N/A	N/A
RLM1/YPL089C*	20	Myr	TOXIC	-	N/A
SMP1 / YBR182C*	20, 107	YeastMine	TOXIC	+	+
SSN2/YDR443C	608[P]	Myr	-	N/A	N/A
YHP1/YDR451C*	180, 182	Myr	-	N/A	N/A

Mitotic Cell Cycle

BCK2/YER167W	12, 38, 373, 430	YeastMine	TOXIC	-	N/A
ESC2/YDR363W	114, 143, 145	YeastMine	-	N/A	N/A
PTK2/YJR059W	59[P], 82, 91, 171, 275	Myr, YeastMine	+	N/A	N/A
SET3/YKR029C	236, 405, 428	YeastMine	-	N/A	N/A
SWI4/YER111C	816[P]	Myr, YeastMine	-	N/A	N/A

VHS2/YIL135C	316, 318, 325^{P}	Myr, Casp	-	N/A	N/A
ZDS1/YMR273C*	78, 370	AbA, YeastMine	-	N/A	N/A
ZDS2/YML109W	183, 267, 345	YeastMine	-	N/A	N/A

Protein Phosphorylation

HAL5/YJL165C	17^{P}, 217^{P}, 233	YeastMine	-	N/A	N/A
KIN1/YDR122W	652, 791^{P}, 879, 986^{P}	YeastMine	+	N/A	N/A
KIN2/YLR096W	665^{P}, 818, 1020	Myr	-	N/A	N/A
KSP1/YHR082C	594, 827^{P}, 884^{P}	Myr, AbA, YeastMine	TOXIC	-	N/A
NPR1/YNL183C	125^{P}, 255^{P}, 257^{P}, 317^{P}	YeastMine	++++	N/A	-
SKY1/YMR216C	383^{P}	Myr, YeastMine	-	N/A	N/A
YAK1/YJL141C	128^{P}, 206, 240	Myr, Casp, YeastMine	-	N/A	N/A
YPL150W	371^{P}, 452, 890	YeastMine	-	N/A	N/A

Lipid Metabolic Process

ADR1/YDR216W	180, 230^{P}, 756	Myr, AbA	-	N/A	N/A
CDC1/YDR182W*	9	N/A	-	N/A	+
CKI1/YLR133W	14^{P}, 25^{P}, 30^{P}	Myr, AbA, YeastMine	-	N/A	N/A

GPT2 / YKR067W	27, 652	Myr	+++	N/A	+
LAC1 / YKL008C*	23, 24	Myr, YeastMine	+++	N/A	+
LAG1 / YHL003C	24[P]	Myr, YeastMine	+++	N/A	+
LCB3/YJL134W	16[P]	Myr, YeastMine	-	N/A	+

Cellular Ion Homeostasis and Transport

AVT3/YKL146W	55, 59[P], 172, 174	Myr, AbA, YeastMine	-	N/A	N/A
CCH1 / YGR217W	146, 148, 347	YeastMine	-	N/A	+
FPS1 / YLL043W	147, 181, 185, 570[P]	Myr, YeastMine	+++++	N/A	+
MNR2/YKL064W	165, 620, 621, 826	AbA	-	N/A	N/A
NHA1/YLR138W*	544, 830	Myr, YeastMine	-	N/A	N/A
PPZ1/YML016C	122, 203, 250[P]	Myr, YeastMine	TOXIC	-	N/A

Translation

DED1/YOR204W	84, 576[P]	YeastMine	-	N/A	N/A
HCR1/YLR192C*	223	Myr, AbA, YeastMine	-	N/A	N/A
HEF3/YNL014W*	898	Myr, AbA, YeastMine	-	N/A	N/A

RPL3/YOR063W	24[P], 337	Myr, AbA, YeastMine	-	N/A	N/A
SUI2/YJR007W*	58	Myr	-	N/A	N/A
TEF1/YPR080W*	72[P]	Myr	-	N/A	N/A

Cell Wall Organization or Biogenesis

BPH1/YCR032W	1334, 1336, 1963	Casp	-	N/A	N/A
CSR2/YPR030W	61, 103, 525, 987	Myr	-	N/A	N/A
ROM2/YLR371W	76[P], 193[P], 396	YeastMine	-	N/A	N/A
SSD1/YDR293C	164[P], 482[P], 503	Myr, AbA, YeastMine	TOXIC	-	N/A

Golgi Vesicle Transport

BRE5/YNR051C	398[P]	Myr, YeastMine	+++	N/A	-
EXO84/YBR102C	76, 313, 494, 554	YeastMine	-	N/A	N/A
MUK1 / YPL070W	173, 184[P], 185[P]	Myr	+++	N/A	+/-
RGP1/YDR137W	220, 364[P], 450, 452	YeastMine	-	N/A	N/A

Signaling

IRA2/YOL081W	882, 884, 1578, 1745, 3069	YeastMine	N/A	N/A	N/A
GIS3/YLR094C*	249, 333	Myr, AbA	-	N/A	N/A

MDS3/YGL197W	757, 824, 842, 851, 1204	Myr, AbA, YeastMine	+++	N/A	-
SYT1/YPR095C	277[P], 410, 728	YeastMine	N/A	N/A	N/A

DNA Replication

CDC13/YDL220C	314, 333[P]	YeastMine	TOXIC	-	N/A
CTI6/YPL181W	155, 216[P]	Myr, YeastMine	-	N/A	N/A
RIM4/YHL024W	93, 429, 525, 607	YeastMine	-	N/A	N/A

Endocytosis

ALY2/YJL084C	166[P], 201, 225, 803	Myr	-	N/A	N/A
ROD1 / YOR018W	563, 617, 807, 823	Myr	+++	N/A	+/-
ROG3/YFR022W	425, 584, 718	YeastMine	-	N/A	N/A

Other

FRT1/YOR324C	167, 201, 203, 228[P], 385	Myr, YeastMine	-	N/A	N/A
HER1/YOR227W	28[P], 102[P], 157[P]	Myr, AbA	TOXIC	-	+
YSP2 / YDR326C	326, 518, 1237	Myr, YeastMine	+++	N/A	+

RNA Catabolic Process

JSN1/YJR091C	174, 275^{P}, 600	YeastMine	-	N/A	N/A
PUF2/YPR042C	55, 143, 246, 902	Myr	N/A	N/A	N/A
Cytokinesis					
CYK3/YDL117W	159, 207^{P}, 746	AbA, YeastMine	+++	N/A	-
Chromosome Segregation					
DSN1/YIR010W	240, 250^{P}	YeastMine	-	N/A	N/A
Peroxisome Organization					
PEX31 / YGR004W	432^{P}	YeastMine	++	N/A	+
Pseudohyphal Growth					
PAM1/YDR251W	471, 553^{P}, 625	Myr, AbA, Casp, YeastMine	-	N/A	N/A
Response to Starvation					
ATG21 / YPL100W	191, 237^{P}	Myr	+++	N/A	+

[a]Genes that are not bioinformatically predicted Ypk1 substrates, but contain Ypk1 motifs and were included in this study are marked with an asterisk. SDL assay results are listed for each bioinformatically predicted Ypk1 substrate. The scoring system reports growth phenotypes of the *ypk1-as ypk2Δ* strain transformed with the indicated P_{GAL1}-SUBSTRATE plasmid upon overexpression on galactose with varying levels of 3-MB-PP1-imposed Ypk1-as inhibition. A growth phenotype is defined as at least 1 serial dilution spot less growth than YCpLG-GFP control at the given 3-MB-PP1 concentration. A strong growth phenotype is defined as no

growth at the given 3-MB-PP1 concentration. (+++++) indicates a growth phenotype with no 3-MB-PP1. (++++) is a strong growth phenotype on 1 μM 3-MB-PP1. (+++) indicates a growth phenotype on 1 μM 3-MB-PP1. (++) is defined as no phenotype on 1 μM 3-MB-PP1, but a strong growth phenotype on 2 μM 3-MB-PP1. (+) indicates no phenotype on 1 μM 3MBPP1, but a detectable growth phenotype on 2 μM 3-MB-PP1. (-) indicates no growth phenotype at any concentration of 3-MB-PP1 tested. TOXIC indicates overexpression of the putative substrate on galactose-containing media was deleterious to growth even in the wild-type control strain (BY4741). These toxic genes were then tested for Ypk1 dosage rescue (for details, see Materials and Methods); here, (+) indicates that Ypk1 overexpression could at least partially rescue the overexpression toxicity of the indicated gene and (-) indicates that Ypk1 overexpression could not rescue the overexpressiion toxicity. Lastly, the results of testing the indicated purified predicted Ypk1 target as a substrtate in the *in vitro* protein kinase assay with purified Ypk1-as; here, (+) indicates that Ypk1-as- dependent (3-MB-PP1 inhibitable) incorporation was detectable for the substrate at a level comparable seen for incorporation into the positive control (the known Ypk1 substrate, GST-Orm1(1-85); (+/-) indicates that readily detectable Ypk1-as-dependent incorporation was found, but at a level lower than that seen for an equivalent amount of GST-Orm1(1-85) protein. (N/A) indicates that the indicated gene product was not tested in the indicated assay.

[b]The SDL assay was performed with a plasmid constitutively overexpressing *CCH1* under the *TDH3* promoter [pBCT-CCH1H, (Iida et al. 2007)], as our efforts to generate a P_{GAL1}-*CCH1* vector failed.

Table 2. *Saccharomyces cerevisiae* strains used in this study

Strain	Genotype	Source/reference
BY4741	*MAT***a** *his3Δ1 leu2Δ0 met15Δ0 ura3Δ0*	Research Genetics, Inc.

BY4742	*MAT***α** *his3*Δ*1 leu2*Δ*0 lys2*Δ*0 ura3*Δ*0*	Research Genetics, Inc.
yAM135-A	BY4741 Ypk1(L424A)::*URA3- ypk2*Δ*::* KanMX4	This study
JTY6142	BY4741 *ypk1*Δ*::*KanMX4	Research Genetics, Inc.
yAM120-A	BY4741 *ypk2*Δ*::*KanMX4	This study
yAM159-A	BY4741 3xFLAG-Lag1::*LEU2*	This study
yAM163-A	BY4741 3xFLAG-Lag1(S23A S24A)::*LEU2*	This study
yAM165-A	BY4742 3xHA-Lac1::*HIS3*	This study
yAM166-A	BY4742 3xHA-Lac1 (S23A S24A)::*HIS3*	This study
JTY5574	BY4741 *cna1*Δ*::*KanMX4 *cna2*Δ*::*KanMX4	M.S. Cyert, Stanford Univ.
YDB379	BY4741 Ypk1-3xFLAG::natNT2	J.S. Weissman, Univ. of California, San Francisco
yAM205-A	BY4742 Lac1::*LEU2* Lag1::*LEU2*	This study
yAM207-B	BY4742 Lac1(S23A S24A)::*LEU2* Lag1(S23A S24A)::*LEU2*	This study
yAM210	BY4742 Lac1(S23E S24E)::*LEU2* Lag1(S23E S24E)::*LEU2*	This study
yGT12	BY4742 *LYS2*$^{+}$ Lac1::*LEU2* Lag1::*LEU2* *lcb3*Δ::natNT2	This study
yGT13	BY4742 *LYS2*$^{+}$ Lac1(S23A S24A)::*LEU2* Lag1(S23A S24A)::*LEU2 lcb3*Δ::natNT2	This study
yGT14	BY4742 *LYS2*$^{+}$ Lac1(S23E S24E)::*LEU2* Lag1(S23E S24E)::*LEU2 lcb3*Δ::natNT2	This study

yAM168	BY4741 3xHA-Lac1::*HIS3* 3xFLAG-Lag1::*LEU2*	This study
yAM184	BY4741 3xHA-Lac1(S23A S24A)::*HIS3* 3xFLAG-Lag1(S23A S24A)::*LEU2*	This study
yAM192-A	BY4741 *MET15*$^{+}$ 3xHA-Lac1(S23E S24E)::*HIS3* 3xFLAG-Lag1(S23E S24E)::*LEU2*	This study
yKL4	BY4741 *TOR2*$^{+}$::Hyg^{r}	Kristin Leskoske, this lab
yKL5	BY4741 Tor2(L2178A)::Hyg^{r}	Kristin Leskoske, this lab

Table 3. Plasmids used in this study.

Plasmid	**Description**	**Source/reference**
pGEX6P-1	GST tag, bacterial expression vector	GE Healthcare, Inc.

pGEX4T-1	GST tag, bacterial expression vector	GE Healthcare, Inc.
YCpLG	*CEN*, *LEU2*, P_{GAL1} vector	(Bardwell et al. 1998)
BG1805	*2µm*, *URA3*, P_{GAL1}, C-terminal tandem affinity (TAP) tag vector	Open Biosystems, Inc.
pRS313	*CEN*, *HIS3*, vector	(Sikorski and Hieter 1989)
pRS316	*CEN*, *URA3*, vector	(Sikorski and Hieter 1989)
pRS416	*CEN*, *URA3*, vector	(Sikorski and Hieter 1989)
pBC111	*CEN, LEU2*, vector	(Iida et al., 2007)
CHp282	pRS416 P_{MET25}-GFP	Chau Huynh, this laboratory
pLB215	pRS416 P_{MET25}-Ypk1	(Niles et al. 2012)
pAX53	pRS416 P_{MET25}-Ypk1(K376A)	This study
pAX50	BG1805 Ypk1(L424A)	This study
pFR203	pGEX4T-1 Orm1(1-85)	(Roelants et al. 2011)
pBT6	pGEX6P-1 Fps1(1-255)	This study
pBT7	pGEX6P-1 Fps1(531-669)	This study
pBT12	pGEX6P-1 Smp1	This study
pAX55	pGEX6P-1 Lcb3(1-79)	This study
pAX56	pGEX6P-1 Cdc1(1-41)	This study
pAX58	pGEX6P-1 Her1(1-224)	This study
pAX59	pGEX6P-1 Rts3	This study
pAX62	pGEX6P-1 Fkh1	This study

pAX63	pGEX6P-1 Yhp1	This study
pAX66	pGEX6P-1 YNR014W	This study
pAX67	pGEX6P-1 YHR097C	This study
pAX94	pGEX6P-1 Mds3(545-1016)	This study
pAX131	pGEX4T-1 Lac1(1-76)	This study
pAX132	pGEX4T-1 Lac1(1-76)(S23A S24A)	This study
pFR291	pGEX4T-1 Lag1(1-80)	This study
pAX133	pGEX4T-1 Lag1(1-80)(S23A S24A)	This study
pAX134	pGEX6P-1 Muk1(1-305)	This study
pAX215	pGEX6P-1 Cyk3	This study
pAX223	pGEX6P-1 Gpt2(1-35)	This study
pAX224	pGEX6P-1 Gpt2(570-743)	This study
pAX225	pGEX6P-1 Bre5	This study
pAX226	pGEX6P-1 Npr1(1-437)	This study
pAX227	pGEX6P-1 Pal1	This study
pAX228	pGEX6P-1 Ysp2(97-665)	This study
pAX229	pGEX6P-1 Ysp2(1072-1282)	This study
pAX230	pGEX6P-1 Atg21	This study
pAX231	pGEX6P-1 Pex31(250-462)	This study
pAX136	pRS313 P_{LAC1}-3xHA-Lac1	This study
pFR273	pRS316 P_{YPK1}-Ypk1(D242A)	(Roelants et al. 2011)
pAX250	pRS313 P_{TPI1}-GFP-Atg8	This study
pBCT-CCH1H	pBC111 P_{TDH3}-Cch1	(Iida et al., 2007)

1236

1237

Figure Legends

Figure 1. A three-part screen to identify likely Ypk1 substrates. (A) The three-part screening strategy to identify Ypk1 substrates is shown schematically as a flow chart. Numbers indicate the number of hits/considered genes at each step in the screen. (B) The bioinformatic approach towards identifying Ypk1 substrates is schematized as a flowchart with each filter as a box. Genes were first filtered by MOTIPS on the basis of having likely phosphorylatable Ypk1 motifs. Subsequently, substrates were filtered by having many Ypk1 motifs or having a Ypk1 site known to be phosphorylated in published data sets. Lastly, genes were filtered by requiring the gene to have a published chemical sensitivity like Ypk1 does, or a published interaction with Ypk1, Ypk1 regulators (TORC2 or PP2A) or sphingolipid biosynthetic machinery.(C) A possible explanation for Ypk1 synthetic dosage lethality interactions is shown. Normally, the cell has enough kinase activity to buffer overexpression of a substrate (Substrate 2), so that essential substrates are regulated and normal growth is unperturbed. However, concurrent decrease in kinase activity coupled with substrate overexpression causes loss of regulation of essential substrate(s) (Substrate 1) leading to observable growth defects. (D) *ypk1-as ypk2Δ* (yAM135 – A) cells were transformed with P_{GAL1}-GFP (negative control), P_{GAL1}-Orm1 or P_{GAL1}-Orm2 (known Ypk1 substrates, positive SDL controls) plasmids. Overnight cultures were then serially diluted onto either dextrose (to repress substrate overexpression) or galatose (to induce substrate overexpression) containing media with increasing concentrations of the Ypk1-as inhibitor 3MBPP1. (E) GST-Orm1(1-85) (pFR203) and GST-Fps1(1-255) (pBT6) were purified from *E. coli* and incubated with [γ-^{32}P]ATP and Ypk1-as, purified from *S. cerevisiae*, in the absence or presence of 3MBPP1. The products were then resolved by SDS/PAGE and analyzed as described in Materials and Methods.

Figure 2. **Lac1 and Lag1, subunits of ceramide synthase, were identified by the screen.** (A) A diagram of the membrane topology of Lac1 and Lag1 derived from (Kageyama-Yahara

and Riezman 2006). Lac1 and Lag1 are experimentally determined to have 6 transmembrane domains. The N terminus of these proteins is cytosolic and therefore accessible for Ypk1 phosphorylation. (B) Diagram of yeast *de novo* sphingolipid biosynthesis derived from (Dickson 2008). Metabolites appear as boxes and enzymes as ovals. Metabolites in green are those directly produced or derived from ceramide synthase while those in red are alternative products at the ceramide synthase branch point. (C) SDL results for Lac1 and Lag1. *ypk1-as ypk2Δ* (yAM135 – A) or wildtype (BY4741) cells were transformed with P_{GAL1}-GFP (negative control), P_{GAL1}-Lac1 or P_{GAL1}-Lag1 plasmids. The SDL assay was then performed as described in Materials and Methods. (D) GST-Lac1(1-76) (pAX131), GST-Lag1(1-80)(pFR29), GST-Lac1(1-76)(S23A S24A)(pAX132) and GST-Lag1(1-80)(S23A S24A)(pAX133) were purified from *E. coli* and Ypk1-as kinase assays were performed as in Figure 1D.

Figure 3. **Ypk1 phosphorylates Lac1 and Lag1 at S23 and S24 *in vivo*.** (A) 3xHA-Lac1 (yAM165-A) 3xHA-Lac1(S23A S24A) (yAM166-A), 3xFLAG-Lag1 (yAM159-A) and 3xFLAG-Lag1(S23A S24A) (yAM163-A) strains were grown exponentially in YPD. Cells were then harvested and whole-cell extracts were prepared. Extracts were split and one fraction was then treated with calf intestinal phosphatase. The extracts resolved by Phos-tag SDS-PAGE and immunoblotted with anti-HA, -FLAG or -Pgk1 (loading control) antibodies. P-Lac1 and P-Lag1 indicate the band corresponding to S23 S24 phosphorylation. * indicates a non-specific band that appears in HA blots of yeast whole cell extracts. (B) Wildtype (BY4741), *ypk1Δ* (JTY6142) and *ypk2Δ* (yAM120 – A) strains were transformed with a plasmid centromeric plasmid encoding 3xHA-Lac1 expressed under control of its endogenous promoter (pAX136). Cells were grown to mid-exponential phase and then treated with a sublethal dose of myriocin (0.625 μM) or methanol (vehicle) for 2 h. Cell extracts were then prepared, resolved by Phos-tag SDS-PAGE and blotted as above in (A). (C) *TOR2* (yKL04) or *tor2-as* (yKL05) strains were transformed with a 3xHA-Lac1 expressing plasmid (pAX136). Cells were grown to mid-

exponential phase and treated with 1 uM BEZ-235 for the indicated times. Cell extracts were then prepared, resolved by Phostag SDS-PAGE and blotted as above in (A).

Figure 4. **Enhanced Ypk1 phosphorylation of Lac1 and Lag1 under sphingolipid and heat stress.** (A) 3xHA-Lac1 (yAM165-A) cells were grown to early exponential phase in YPD. Cultures were then treated with sublethal doses of myriocin (0.625 μM) or methanol (vehicle) or aureobasidin A (1.8 μM) of ethanol (vehicle) for 2 h. (B) 3xHA-Lac1 (yAM165-A) cells were grown to exponential phase in YPD at 30˚C. A sample of this culture was then harvested. The remaining culture was then moved to 42˚C to initiate heat shock and samples were harvested at the indicated time points. Whole cell extracts were prepared from each sample, resolved by Phos-tag SDS-PAGE, and immunoblotted as in Figure 3. P-Lac1 indicates the band corresponding to S23 S24 phosphorylation. * indicates a non-specific band that appears in HA blots of yeast whole cell extracts. (C) *LAC1 LAG1* (yAM205 - A), $Lac1^{SSAA}$ $Lag1^{SSAA}$ (yAM207 - B) and $Lac1^{SSEE}$ $Lag1^{SSEE}$ (yAM210) were grown to exponential phase in YPD. Serial dilutions of each culture were made and spotted on YPD plates containing vehicle or the indicated concentration of myriocin or aureobasidin A. Cells were allowed to grow for 3 days at 30˚C prior to imaging. (D) 3xHA-Lac1::*HIS3* 3xFLAG-Lag1::*LEU2* (yAM168) 3xHA-Lac1(S23A S24A)::*HIS3* 3xFLAG-Lag1(S23A S24A)::*LEU2* ($Lac1^{SSAA}$ $Lag1^{SSAA}$) (yAM184) and 3xHA-Lac1(S23E S24E)::*HIS3* 3xFLAG-Lag(S23E S24E)1::*LEU2* ($Lac1^{SSEE}$ $Lag1^{SSEE}$) (yAM192 – A) cells were grown to mid-exponential phase and then treated with 1.0 uM myriocin or 18.2 nM aureobasidin A for 2h. Whole cell extracts were prepared from each sample, resolved by SDS-PAGE, and immunoblotted as indicated.

Figure 5. **Activation of calcineurin leads to rapid dephosphorylation of Lac1 and Lag1 with affecting Ypk1 function**. (A) Wildtype (BY4741) or *cna1Δ cna2Δ* (JTY5574) strains were transformed with a centromeric plasmid encoding 3xHA-Lac1 expressed under control of its

endogenous promoter (pAX136). Cultures were grown to mid-exponential phase in selective media and then treated with 200 mM $CaCl_2$ for 10 minutes to activate calcineurin. Cultures were then harvested and whole cell extracts were prepared from each sample, resolved by Phos-tag SDS-PAGE, and immunoblotted as in Figure 3. (B) 3xHA-Lac1 (yAM165-A) cells were transformed with a centromeric plasmid encoding the hyperactive TORC2 independent $Ypk1^{D242A}$ allele expressed under its own promoter (pFR273) or vector (pRS316). Cultures were grown in selective media to mid-exponential phase before treatment with 200 mM $CaCl_2$ for 10 min. Cultures were then harvested and whole cell extracts were prepared from each sample, resolved by Phos-tag SDS-PAGE, and immunoblotted as above. (C) 3xFLAG-Ypk1 (YDB379) cells were grown to midexponential phase in YPD. Cultures were treated with or without 200 mM $CaCl_2$ for 10 min. Cells were then harvested and whole extracts prepared. Extracts were resolved by SDS-PAGE and blotted with anti-pSGK(T256), which recognizes Ypk1 T504 activation loop phosphorylation and anti-FLAG antibody (Ypk1 loading control). The blot is representative of triplicate samples and the quantitation of the ratio of pT504/FLAG from these replicates is shown below the blot.

Figure 6. **Ypk1 phosphorylation of Lac1 and Lag1 stimulates ceramide synthase activity**. (A) Cultures of *LAC1 LAG1* (yAM205 - A), $Lac1^{SSAA}$ $Lag1^{SSAA}$ (yAM207 - B) and $Lac1^{SSEE}$ $Lag1^{SSEE}$ (yAM210) strains were grown to mid-exponential phase and then harvested. Sphingolipids were extracted and analyzed as described in Materials and Methods. Values represent the mean of three independent experiments (each performed in triplicate) and error bars represent SEM. (B) Triplicate exponentially-growing cultures of *LAC1 LAG1* (yAM205 - A), $Lac1^{SSAA}$ $Lag1^{SSAA}$ (yAM207 - B) and $Lac1^{SSEE}$ $Lag1^{SSEE}$ (yAM210) were grown overnight and duplicate cultures were diluted to OD_{600} = 1.0. Complex sphingolipids were labeled and analyzed by thin layer chromatography (TLC) as in Materials and Methods. A representative TLC plate is shown with the origin at the bottom of the image. The assigned identity of species

as IPCs and MIPCs was confirmed by pharmacological or genetic inhibition of the production of these species in control cultures (data not shown). Quantification of total complex sphingolipids was performed in ImageJ by integrating the Phosphorimager screen intensity across the lane for each sample and normalized to 1 for the wild-type ceramide synthase samples. (C) *Upper,* ceramide synthase was purified by FLAG immunopurification from 3xHA-Lac1::*HIS3* 3xFLAG-Lag1::*LEU2* (yAM168) 3xHA-Lac1(S23A S24A)::*HIS3* 3xFLAG-Lag1(S23A S24A)::*LEU2* ($Lac1^{SSAA}$ $Lag1^{SSAA}$) (yAM184) and 3xHA-Lac1(S23E S24E)::*HIS3* 3xFLAG-Lag(S23E S24E)1::*LEU2* ($Lac1^{SSEE}$ $Lag1^{SSEE}$) (yAM192 – A) cells. Immunoprecipitates were then split into 3 fractions and *in vitro* ceramide synthase assays (60 min reactions) were performed in triplicate. A small sample of each ceramide synthase assay was resolved by SDS-PAGE and immunoblotted. The signal intensity quantified from the immunoblot was then used to normalize ceramide synthase activity in each sample. *Lower,* ceramide synthase was immunopurified from 3xHA-Lac1::*HIS3* 3xFLAG-Lag1::*LEU2* (yAM168) 3xHA-Lac1(S23A S24A)::*HIS3* or 3xFLAG-Lag1(S23A S24A)::*LEU2* ($Lac1^{SSAA}$ $Lag1^{SSAA}$) (yAM184) cells as above except cultures were treated with 1.0 uM myriocin or methanol vehicle prior to harvesting. Values represent the mean of three independent experiments (each performed in triplicate) and error bars represent SEM. Statistical significance of values (Student's t-test): *, $p = <0.05$, **, $p = <0.009$; and, ***, $p <0.0009$.

Figure 7. **Failure of Ypk1 to upregulate ceramide synthase causes LCBP accumulation that triggers autophagy.** (A) *LAC1 LAG1* (yAM205 - A) or $Lac1^{SSAA}$ $Lag1^{SSAA}$ (yAM207 - B) were transformed with P_{YPK1}-$Ypk1^{D242}$ (shown as Ypk1*) (pFR273) or empty vector pRS316 (E.V.). Transformants were grown strains were grown to exponential phase in synthetic complete media and then diluted to OD_{600}=0.1 and grown in microtiter plates (*lower*) or on agar plates (*upper*). For liquid cultures, each was grown in at least quadruplicate and the error bars indicate the SEM of replicates at each time point. (B) Cells from (A) were grown to mid-

exponential phase in selective synthetic complete media and then harvested. Sphingolipids were extracted and analyzed as described in Materials and Methods. Values represent the mean of three independent experiments (each performed in triplicate) and error bars represent SEM. (C) *LAC1 LAG1 lcb4Δ* (yAM237) or Lac1^{SSAA} Lag1^{SSAA} *lcb4Δ* (yAM238 – A) were transformed with P$_{YPK1}$-Ypk1^{D242} (shown as Ypk1*) (pFR273) and growth experiments performed as in (A). (D) Liquid growth assays were performed as in (A) for *LAC1 LAG1* (yAM205 - A), Lac1^{SSAA} Lag1^{SSAA} (yAM207 - B), Lac1^{SSEE} Lag1^{SSEE} (yAM210), *LAC1 LAG1 lcb3Δ* (yGT12), Lac1^{SSAA} Lag1^{SSAA} *lcb3Δ* (yGT13) and Lac1^{SSEE} Lag1^{SSEE} *lcb3Δ* (yGT14) strains. (E) *LAC1 LAG1* (yAM205 - A) or Lac1^{SSAA} Lag1^{SSAA} (yAM207 - B) or *LAC1 LAG1 lcb3Δ* (yGT12) strains were transformed with P$_{YPK1}$-Ypk1^{D242} (shown as Ypk1*) (pFR273) or pRS316 (E.V.) and additionally P$_{TPI1}$-GFP-Atg8. Growing cultures treated with vehicle or 2 µg/mL rapamycin for 2h and then harvested and whole extracts prepared. Extracts were resolved by SDS-PAGE and blotted with anti-GFP to detect GFP-Atg8 and free GFP arising from GFP-Atg8 autophagic processing and anti-Pgk1 antibody. The blot is representative of triplicate samples and the quantitation of the ratio of free GFP/Pgk1 from these replicates is shown below the blot. (F) *LAC1 LAG1 atg1Δ* (yAM239 - A) or Lac1^{SSAA} Lag1^{SSAA} *atg1Δ* (yAM240 – A) sensitivity to P$_{YPK1}$-Ypk1^{D242} was measured as in (A). (G) Cells from (F) were grown to mid-exponential phase in selective synthetic complete media and then harvested. Sphingolipids were extracted and analyzed as described in (B).

Figure 8. **TORC2-Ypk1 signaling globally activates sphingolipid synthesis, selectively directs flux toward ceramide metabolites, and prevents LCBP cross-talk to the autophagy pathway.** (A) Diagram of yeast *de novo* sphingolipid biosynthesis shown is derived from (Dickson 2008). Enzymes are in ovals. Metabolites are in boxes. Increased color intensity indicates level of metabolite increase in response TORC2-Ypk1 activation. TORC2-Ypk1 signaling globally activates *de novo* sphingolipid biosynthesis via derepression of the SPT

complex (Roelants et al. 2011; Berchtold et al. 2012; Sun et al. 2012), potentially increasing levels of all metabolites. However, Ypk1 also upregulates ceramide synthesis via phosphorylation of Lac1 and Lag1, thus primarily directing this increased flux towards ceramides and away from LCBs and LCBPs. (B) In the absence of Ypk1 mediated ceramide biosynthesis regulation, increased sphingolipid flux raises LCB and LCBP levels. This slows cell growth by activating autophagy. Thus, TORC2-Ypk1 signaling not only activates sphingolipid biosynthesis in response to stress, but also insulates this flux towards ceramides to prevent metabolite mediated crosstalk to the autophagy machinery.

Figure 1

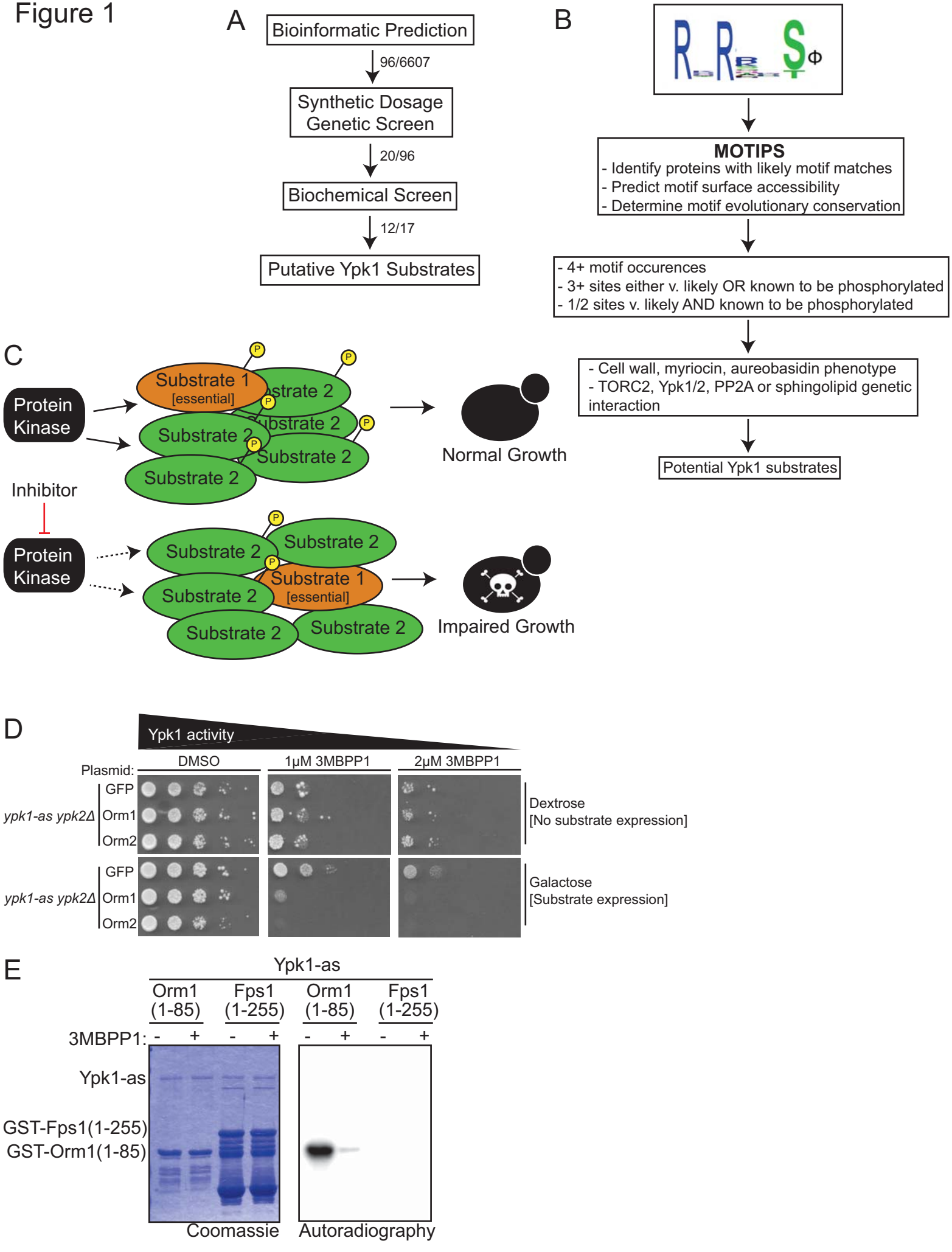
A
Bioinformatic Prediction
96/6607
Synthetic Dosage Genetic Screen
20/96
Biochemical Screen
12/17
Putative Ypk1 Substrates
B
MOTIPS
- Identify proteins with likely motif matches
- Predict motif surface accessibility
- Determine motif evolutionary conservation
- 4+ motif occurences
- 3+ sites either v. likely OR known to be phosphorylated
- 1/2 sites v. likely AND known to be phosphorylated
- Cell wall, myriocin, aureobasidin phenotype
- TORC2, Ypk1/2, PP2A or sphingolipid genetic interaction
Potential Ypk1 substrates
C
Protein Kinase
Substrate 1 [essential]
Substrate 2
Normal Growth
Inhibitor
Impaired Growth
D
Ypk1 activity
Plasmid:
DMSO
1μM 3MBPP1
2μM 3MBPP1
ypk1-as ypk2Δ
GFP
Orm1
Orm2
Dextrose [No substrate expression]
Galactose [Substrate expression]
E
Ypk1-as
Orm1 (1-85)
Fps1 (1-255)
3MBPP1:
Ypk1-as
GST-Fps1(1-255)
GST-Orm1(1-85)
Coomassie
Autoradiography

Figure 2

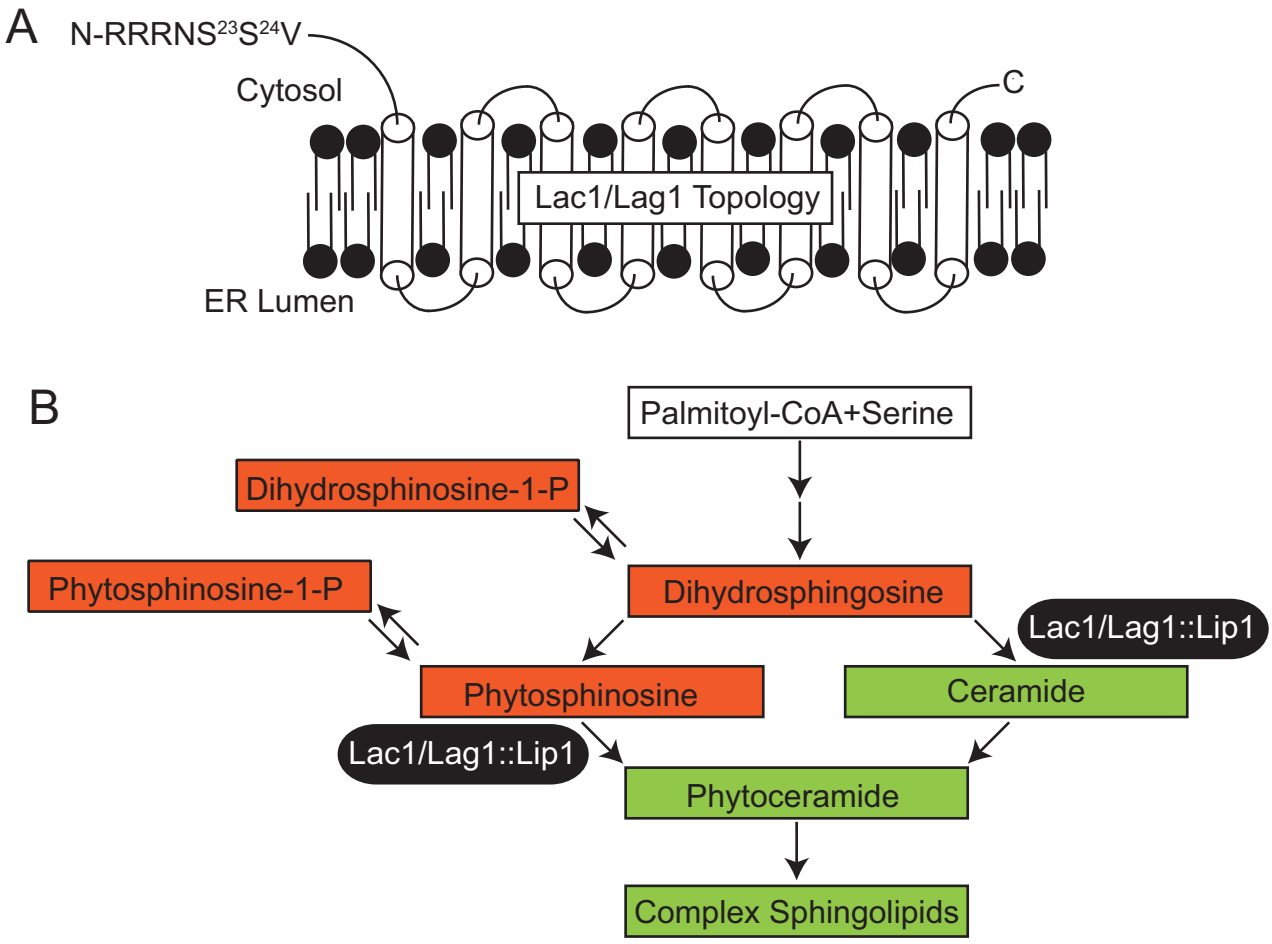
A
N-RRRNS23S24V
Cytosol
C
Lac1/Lag1 Topology
ER Lumen
B
Palmitoyl-CoA+Serine
Dihydrosphinosine-1-P
Phytosphinosine-1-P
Dihydrosphingosine
Lac1/Lag1::Lip1
Phytosphinosine
Ceramide
Lac1/Lag1::Lip1
Phytoceramide
Complex Sphingolipids
C
Plasmid:
DMSO
1μM 3MBPP1
2μM 3MBPP1
Wildtype
GFP
Lac1
Lag1
ypk1-as ypk2Δ
GFP
Lac1
Lag1
D
Ypk1-as
Lac1
Lac1S23A S24A
Lac1
Lac1S23A S24A
3MBPP1: - + - + - + - +
Ypk1
GST-Lac1(1-76)
Coomassie
Autoradiography
Ypk1-as
Lag1
Lag1S23A S24A
Lag1
Lag1S23A S24A
3MBPP1: - + - + - + - +
Ypk1
GST-Lag1(1-80)
Coomassie
Autoradiography

Figure 3

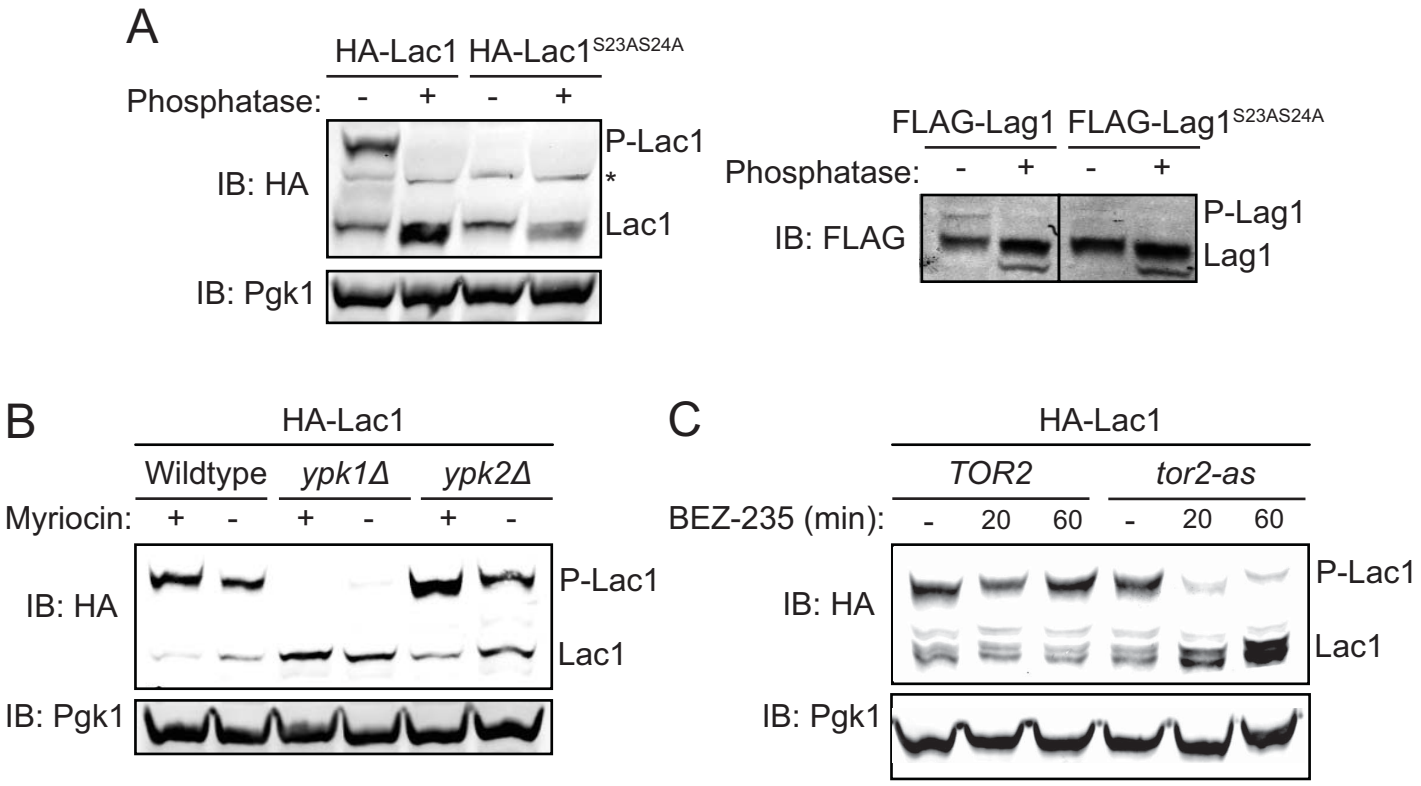
A
HA-Lac1
HA-Lac1S23AS24A
Phosphatase: - + - +
IB: HA
P-Lac1
*
Lac1
IB: Pgk1
FLAG-Lag1
FLAG-Lag1S23AS24A
Phosphatase: - + - +
IB: FLAG
P-Lag1
Lag1
B
HA-Lac1
Wildtype
ypk1Δ
ypk2Δ
Myriocin: + - + - + -
IB: HA
P-Lac1
Lac1
IB: Pgk1
C
HA-Lac1
TOR2
tor2-as
BEZ-235 (min): - 20 60 - 20 60
IB: HA
P-Lac1
Lac1
IB: Pgk1

Figure 4

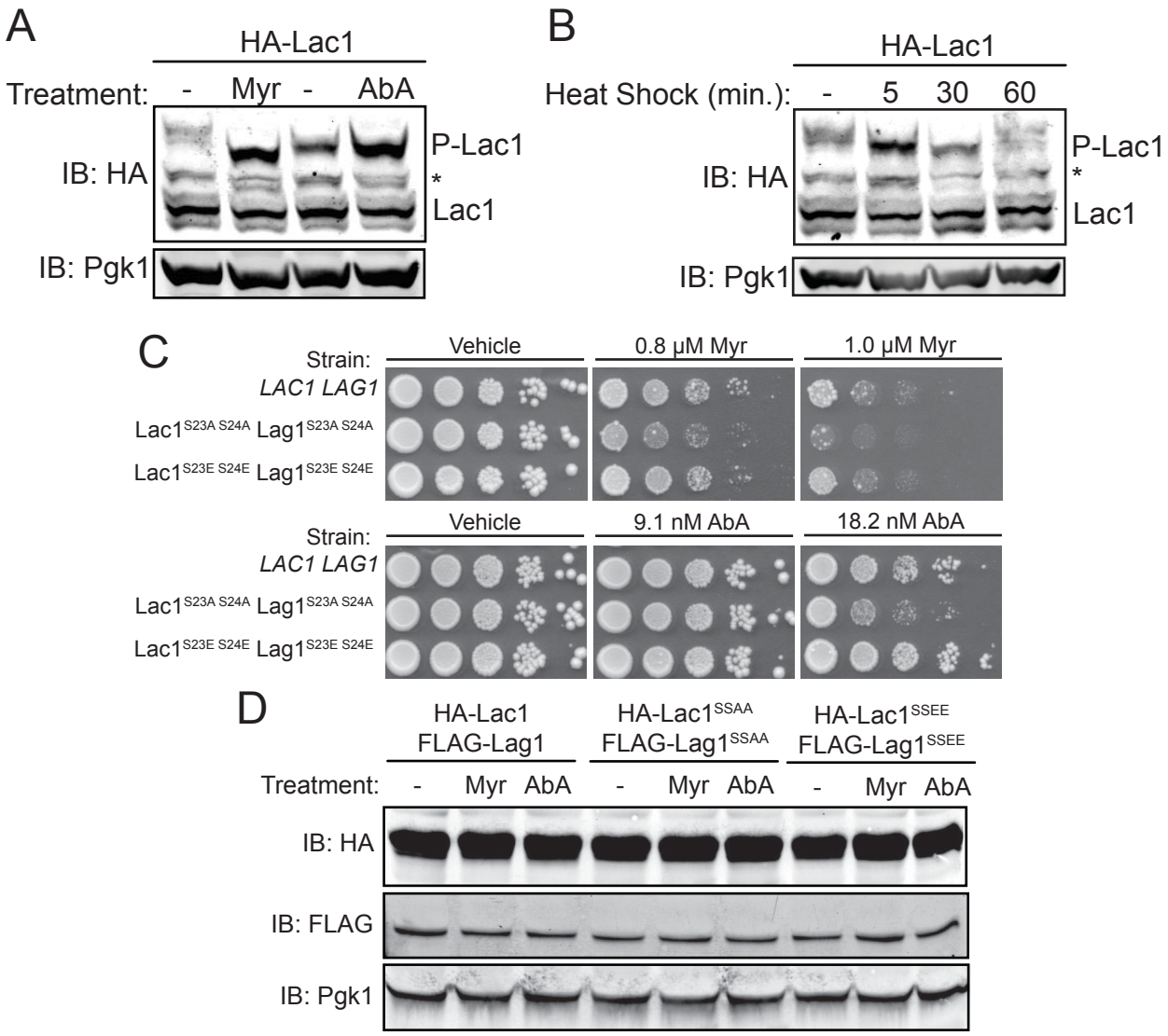
A
HA-Lac1
Treatment: - Myr - AbA
IB: HA
P-Lac1
*
Lac1
IB: Pgk1
B
HA-Lac1
Heat Shock (min.): - 5 30 60
IB: HA
P-Lac1
*
Lac1
IB: Pgk1
C
Strain:
LAC1 LAG1
Lac1S23A S24A Lag1S23A S24A
Lac1S23E S24E Lag1S23E S24E
Vehicle
0.8 μM Myr
1.0 μM Myr
Strain:
LAC1 LAG1
Lac1S23A S24A Lag1S23A S24A
Lac1S23E S24E Lag1S23E S24E
Vehicle
9.1 nM AbA
18.2 nM AbA
D
HA-Lac1
FLAG-Lag1
HA-Lac1SSAA
FLAG-Lag1SSAA
HA-Lac1SSEE
FLAG-Lag1SSEE
Treatment: - Myr AbA - Myr AbA - Myr AbA
IB: HA
IB: FLAG
IB: Pgk1

Figure 5

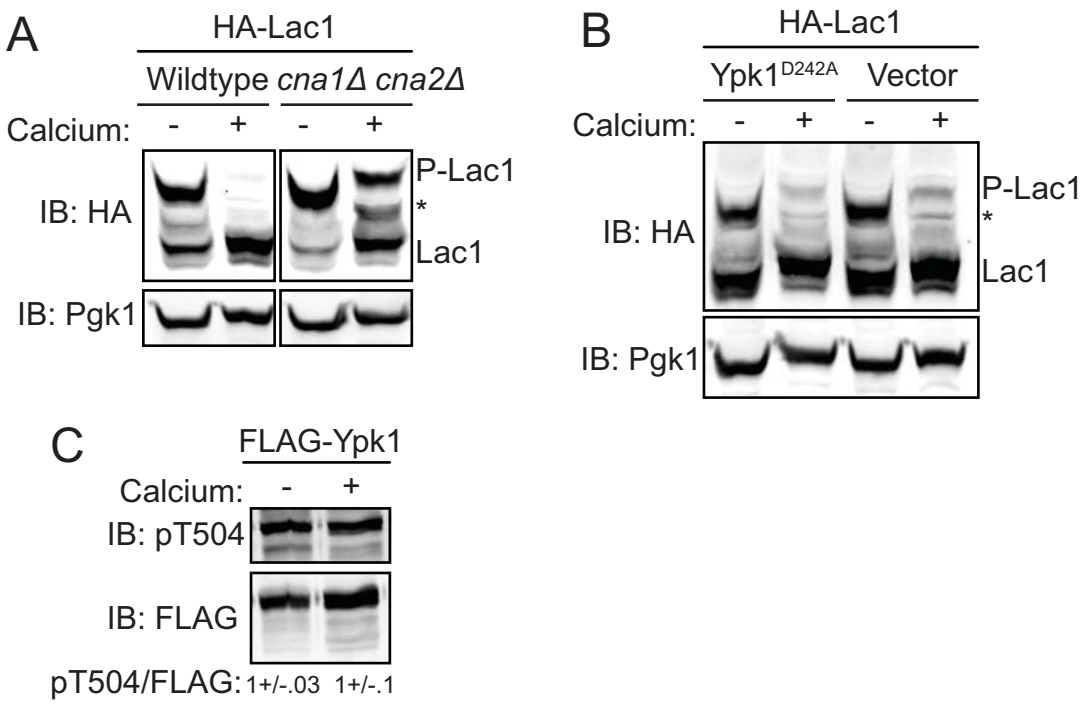
A
HA-Lac1
Wildtype
cna1Δ cna2Δ
Calcium: - + - +
IB: HA
P-Lac1
*
Lac1
IB: Pgk1
B
HA-Lac1
Ypk1D242A
Vector
Calcium: - + - +
IB: HA
P-Lac1
*
Lac1
IB: Pgk1
C
FLAG-Ypk1
Calcium: - +
IB: pT504
IB: FLAG
pT504/FLAG: 1+/-.03 1+/-.1

Figure 6

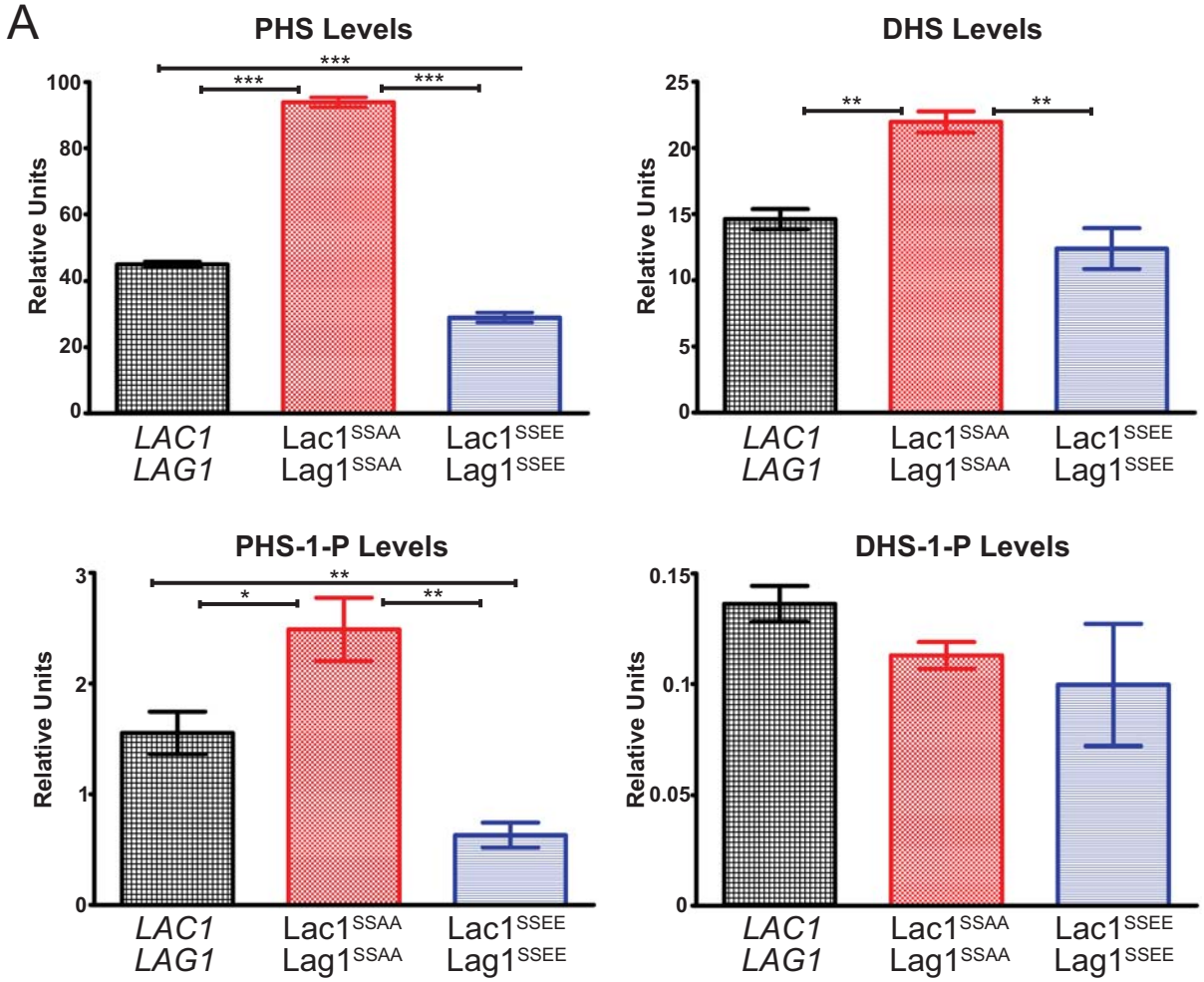
A
PHS Levels
DHS Levels
PHS-1-P Levels
DHS-1-P Levels
Relative Units
LAC1 LAG1
Lac1SSAA Lag1SSAA
Lac1SSEE Lag1SSEE

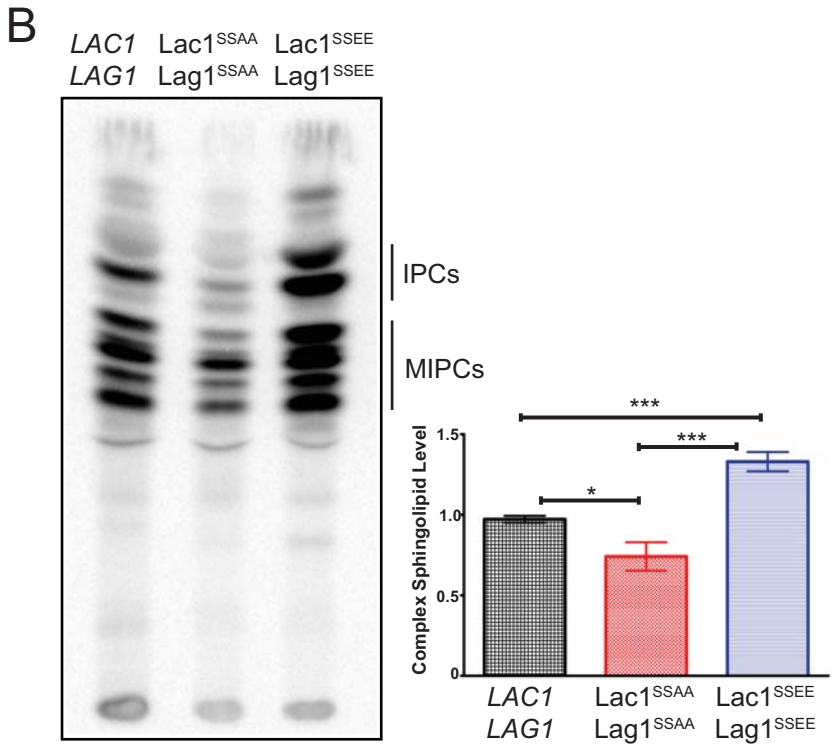
B
LAC1 LAG1
Lac1SSAA Lag1SSAA
Lac1SSEE Lag1SSEE
IPCs
MIPCs
Complex Sphingolipid Level

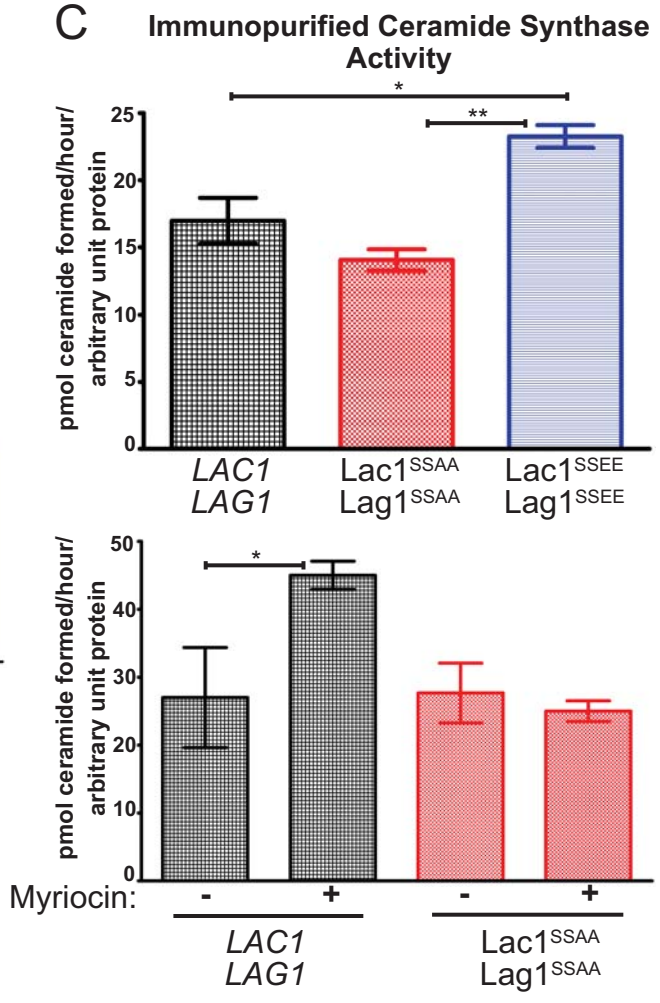
C
Immunopurified Ceramide Synthase Activity
pmol ceramide formed/hour/ arbitrary unit protein
Myriocin:
LAC1 LAG1
Lac1SSAA Lag1SSAA

Figure 7

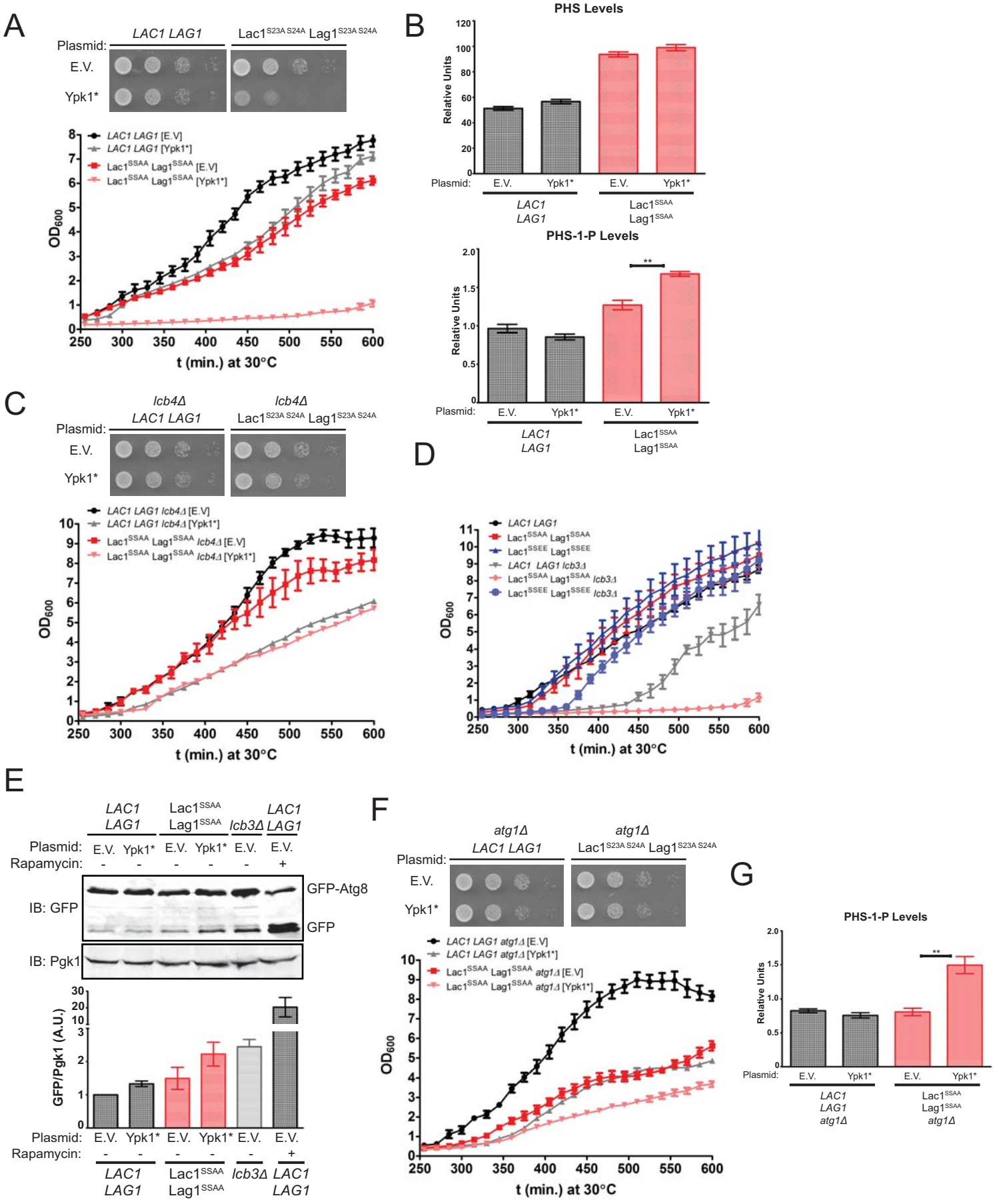
A
Plasmid:
LAC1 LAG1
Lac1S23A S24A Lag1S23A S24A
E.V.
Ypk1*
LAC1 LAG1 [E.V]
LAC1 LAG1 [Ypk1*]
Lac1SSAA Lag1SSAA [E.V]
Lac1SSAA Lag1SSAA [Ypk1*]
OD600
t (min.) at 30°C
B
PHS Levels
Relative Units
Plasmid:
E.V.
Ypk1*
LAC1
LAG1
Lac1SSAA
Lag1SSAA
PHS-1-P Levels
**
C
lcb4Δ
LAC1 LAG1
lcb4Δ
Lac1S23A S24A Lag1S23A S24A
LAC1 LAG1 lcb4Δ [E.V]
LAC1 LAG1 lcb4Δ [Ypk1*]
Lac1SSAA Lag1SSAA lcb4Δ [E.V]
Lac1SSAA Lag1SSAA lcb4Δ [Ypk1*]
D
LAC1 LAG1
Lac1SSAA Lag1SSAA
Lac1SSEE Lag1SSEE
LAC1 LAG1 lcb3Δ
Lac1SSAA Lag1SSAA lcb3Δ
Lac1SSEE Lag1SSEE lcb3Δ
E
LAC1
LAG1
Lac1SSAA
Lag1SSAA
lcb3Δ
LAC1
LAG1
Rapamycin:
IB: GFP
GFP-Atg8
GFP
IB: Pgk1
GFP/Pgk1 (A.U.)
F
atg1Δ
LAC1 LAG1
atg1Δ
Lac1S23A S24A Lag1S23A S24A
LAC1 LAG1 atg1Δ [E.V]
LAC1 LAG1 atg1Δ [Ypk1*]
Lac1SSAA Lag1SSAA atg1Δ [E.V]
Lac1SSAA Lag1SSAA atg1Δ [Ypk1*]
G
PHS-1-P Levels
LAC1
LAG1
atg1Δ
Lac1SSAA
Lag1SSAA
atg1Δ

Figure 8

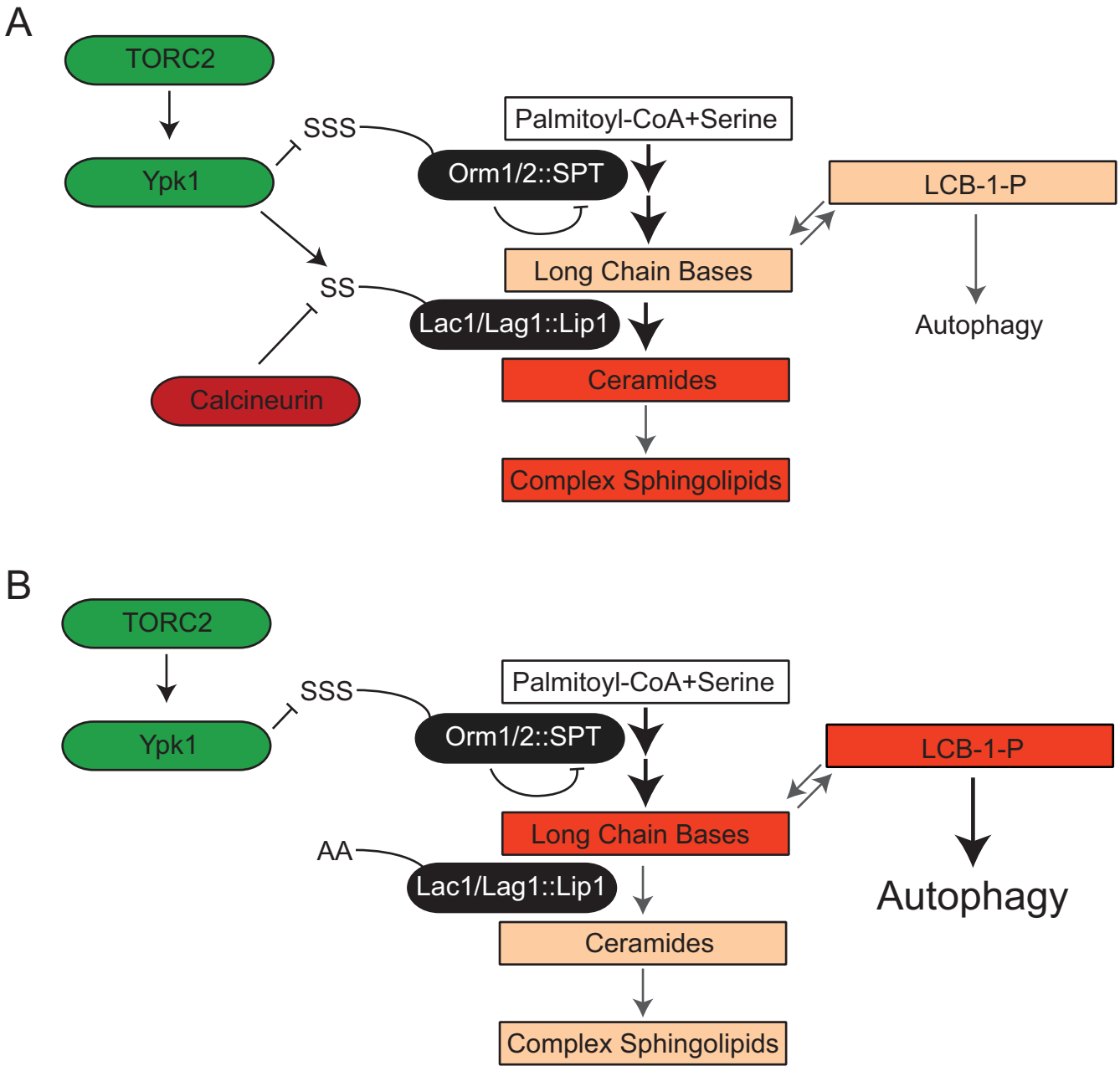
A
TORC2
Ypk1
SSS
Palmitoyl-CoA+Serine
Orm1/2::SPT
LCB-1-P
Long Chain Bases
SS
Lac1/Lag1::Lip1
Autophagy
Calcineurin
Ceramides
Complex Sphingolipids
B
TORC2
Ypk1
SSS
Palmitoyl-CoA+Serine
Orm1/2::SPT
LCB-1-P
Long Chain Bases
AA
Lac1/Lag1::Lip1
Autophagy
Ceramides
Complex Sphingolipids